Estimating Storm-Induced Dune Erosion and Overtopping along U.S. West Coast Beaches

Citation	Mull, J., & Ruggiero, P. (2014). Estimating storm-induced dune erosion and overtopping along US West Coast beaches. Journal of Coastal Research, 30(6), 1173-1187. doi:10.2112/JCOASTRES-D-13-00178.1
DOI	10.2112/JCOASTRES-D-13-00178.1
Publisher	Coastal Education and Research Foundation
Version	Accepted Manuscript
Terms of Use	http://cdss.library.oregonstate.edu/sa-termsofuse

Estimating Storm-Induced Dune Erosion and Overtopping along U.S. West Coast Beaches

Jeremy Mull[1,2] and Peter Ruggiero[3]

Submitted to: Journal of Coastal Research

[1] *Department of Civil and Construction Engineering, Oregon State University*
Corvallis, Oregon 97331, USA
[2]*Current Address:*
AECOM
710 Second Avenue, Seattle 98104, USA; 541-908-9040
jeremy.mull@aecom.com

[3] *College of Earth, Ocean, and Atmospheric Sciences, Oregon State University*
Corvallis, Oregon 97331, USA; 541-737-1239
pruggier@coas.oregonstate.edu

ABSTRACT

Coastal foredunes protect lives, infrastructure, and ecosystems during severe storms. A range of approaches, ranging from simple (*e.g.*, geometric) to complex (*e.g.*, process-based) predictive models, have been developed to quantify overtopping and foredune retreat during storms. At present, however, there is no widely accepted approach for assessing the vulnerability of coastal foredunes to erosion and overtopping hazards. Because different coastal regions have distinct storm and geomorphic characteristics, models need to be assessed and possibly adapted before they can be successfully applied to each unique region. In this study, we apply a total water level model and three simple foredune erosion models and assess their suitability for U.S. west coast vulnerability analyses. The erosion models include a geometric model, an equilibrium profile model, and a wave impact model. We discuss the assumptions required to implement each model and force them with hydrodynamic conditions associated with a large-scale laboratory dune erosion experiment and a major winter storm approximately equivalent to the 30-yr return period total water level event in the U.S. Pacific Northwest. The models are each applied with beach and foredune characteristics extracted from airborne topographic lidar data collected along the coasts of Oregon and Washington. Sensitivity tests reveal distinct differences in model dependence on beach slope, a critical parameter in determining storm water level elevations and ultimately the extent of foredune retreat. Without detailed, reliable field observations of storm-induced dune erosion from the region, the accuracy of each model is determined using results of the dune erosion experiment. Estimates of both overtopping and erosion extent are normalized by foredune dimensions enabling comparisons of relative vulnerability between different reaches of coast.

ADDITIONAL INDEX WORDS: *Coastal vulnerability, geomorphology, dune erosion, overtopping*

INTRODUCTION

Foredunes directly serve coastal communities by protecting lives, infrastructure, and ecosystems from inundation and erosion during severe storms (*e.g.*, Cooper, 1958; Komar *et al.*, 1999; Sallenger, 2000; Seabloom *et al.*, 2013; Stockdon, Doran, and Sallenger, 2009; Stockdon *et al.*, 2007). While some coastal locations are backed by multiple lines of dunes, it is foredunes, or primary dunes, that represent the first line of defense against coastal flooding and erosion for backing properties and infrastructure (Cooper, 1958; Kriebel and Dean, 1993; Stockdon, Doran, and Sallenger, 2009).

Sallenger (2000) developed a simple storm impact scale that elegantly classifies the potential impacts of storm water levels on beaches and foredunes into four distinct regimes. The swash, collision, overtopping, and inundation regimes are distinguished by storm-induced water levels relative to relevant foredune characteristics. During hurricanes and large extratropical storms, dune-backed beaches along the U.S. east and Gulf coasts can reach the overtopping and inundation regimes of the Sallenger (2000) scale due to relatively large storm surge (Stockdon, Doran, and Sallenger, 2009; Stockdon *et al*. 2007), occasionally leading to the complete destruction of foredunes and backshore properties. Along the U.S. west coast, however, storm surge is limited due to the geometry of the shelf (*e.g.*, Bromirski *et al.*, 2003) and foredunes are often relatively tall compared to high water levels. Therefore, U.S. west coast foredunes are typically in the collision regime during storms resulting in some areas being particularly susceptible to erosion with inundation being relatively rare.

Our ultimate aim is to develop approaches for assessing the vulnerabilities of U.S. west coast beaches to foredune overtopping and erosion during severe storm events and to compare these hazards throughout the region. Here we focus on the U.S. Pacific Northwest (PNW), which has some of the largest coastal dune systems in the country with dune-backed beaches covering approximately 45% of the Oregon and Washington coastlines (Figure 1; Cooper, 1958; Hacker *et al.*, 2012). The dunes in the PNW are part of a dynamic coastal system that includes relatively large waves (*e.g.*, Allan and Komar, 2002), typically dissipative beaches, and high seasonal-interannual-decadal variability in nearshore, beach, and foredune geomorphology (*e.g.*, Ruggiero *et al.*, 2005). Dune erosion and overtopping has been documented for coastal communities throughout this region (Allan and Priest, 2001; 2002; Komar *et al.*, 1999), however the processes which drive foredune evolution in the PNW, and ultimately impact coastal vulnerability, are not entirely understood. Accurate methods for predicting storm induced overtopping and erosion will aid coastal planners as they make decisions on how best to manage coastal dune systems now and in the future.

The primary purpose of this paper is to compare three simple, yet fundamentally different, foredune erosion models and assess their appropriateness in estimating foredune erosion along the U.S. west coast. We first present our methodology, modified from those presented by Stockton *et al.* (2009), for extracting relevant morphometric parameters from airborne topographic lidar data for model application. We then discuss the assumptions inherent in the total water level (TWL) and foredune erosion models and the methodologies used to apply them to three distinct littoral cells in the PNW. The computationally simple erosion models include the Komar *et al.* (1999) geometric model (hereinafter referred to as K99), the Kriebel and Dean (1993) equilibrium profile model (hereinafter referred to as KD93), and the Larson, Erikson, and Hanson (2004) wave impact model (hereinafter referred to as L04). While more complex process-based foredune erosion models (*e.g.*, XBEACH, Roelvink *et al.*, 2007) are available for application to relatively small areas, they require detailed information regarding hydrodynamic conditions, sediment characteristics, and nearshore bathymetry. In contrast, the one-dimensional (1-D) erosion models described here do not require such detail and can be applied with only a few hydrodynamic variables, morphometrics, and parameterized sediment characteristics derived from lidar data. While the simple 1-D models do not necessarily capture detailed processes, such as morphological feedbacks between storm water levels and beach and dune evolution during storms, they can easily be applied to large areas and are potentially appropriate for regional scale coastal vulnerability analyses.

Unfortunately, and unlike the U.S. east and Gulf coasts (*e.g.*, Stockdon *et al.*, 2007), there are virtually no detailed littoral cell-scale field observations of foredune erosion during major winter storms in the PNW. This obviously limits our ability to critically test, calibrate, and verify dune erosion models for specific application to the U.S west coast. However, since there is significant societal interest in quantified estimates of potential dune retreat during storms, here we investigate model sensitivities over the range of parameter space common to the PNW. In addition, we use the results of a large-scale laboratory dune erosion experiment to contextualize the sensitivities of the various models. Finally, to expedite the synthesis of the model results, we develop indices in which predicted foredune retreat distances and overtopping estimates are normalized by foredune dimensions to quantify the relative vulnerability to erosion and overtopping throughout the region.

METHODS

The methods to calculate overtopping and erosion are assessed with a physical scale dune erosion experiment and for the PNW storm event 'of record' using geomorphic data, estimates of the wave and water level conditions, and three simple 1-D dune erosion models. Below we describe the experiment, methodologies developed for extracting morphometrics from lidar data as well as the input data and approaches required for applying the various dune erosion models.

Storm Input Conditions

Estimates of TWL achieved on beaches are used to assess the possibility of dune overtopping as well as in the application of each of the dune erosion models. Computing the TWL involves the summation of the predicted astronomical tides, the non-tidal factors that alter the measured tides from those predicted, and the runup levels of the waves on the beach (Ruggiero *et al.*, 2001). Estimates of the (hourly) TWL achieved on beaches (above NAVD88) are taken as

$$TWL = \eta + \eta' + R_2 \quad (1)$$

where η is the astronomical (predicted) tide and η' is the non-tidal residual which we assume to be dominated by storm surge (Allan and Komar, 2002; Ruggiero *et al.*, 2001). It is important to note that measured tidal elevations include both the predicted tidal elevations and non-tidal residuals so that they constitute the still water level (SWL, $\eta + \eta'$). R_2 is the 2% exceedence wave runup height (setup plus swash), or the elevation that 2% of the individual swash events will exceed given specific offshore wave conditions. R_2 is a statistical representation of extreme wave runup based on field observations by Holman (1986), Ruggiero *et al.* (2001), and Stockdon *et al.* (2006) and is commonly used in coastal vulnerability analyses. After Stockdon *et al.* (2006), deepwater significant wave heights, H_0, and wave lengths, L_0, are combined with the backshore beach slope, *tan* β_b, to determine the 2% exceedence wave runup height at each profile.

$$R_2 = 1.1\left(0.35tan\beta_b(H_0L_0)^{1/2} + \frac{\left[H_0L_0\left(0.563tan^2\beta_b+0.004\right)^{1/2}\right]}{2}\right) \quad (2)$$

This equation was developed in part with wave runup data from the PNW (Ruggiero *et al.*, 2001; 2004; Stockdon *et al.*, 2006) and is parameterized similarly to the equation developed by Larson, Erikson, and Hanson (2004) to estimate wave runup elevations in a wave tank with constant beach slope and the root-mean-square wave height (H_{rms}) (Palmsten and Holman, 2012). We use peak spectral periods (T_p) and the linear wave theory dispersion relationship to obtain the deep water equivalent significant wave heights for substitution into Eq. 2. The deepwater wave lengths are assumed to be $L_0=(gT_p^2)/(2\pi)$ where g is the acceleration of gravity.

If the TWL exceeds the dune crest elevation (*dhigh*) at any point during the storm, the profile is in the overtopping regime of the Sallenger (2000) storm impact scale, the severity of which is ultimately a function of overtopping volume (Cox and Machemehl, 1986). If the TWL exceeds the dune toe elevation (*dtoe*) during the storm, the profile is in the collision regime, dune erosion is expected, and one of several dune erosion models can be used to quantify the potential coastal change.

Laboratory Experiment

The TWL and wave runup formulations, and ultimately the three erosion models, are first applied with laboratory data from a dune erosion experiment. Experiments were conducted in the large wave flume of the O.H. Hinsdale Wave Research Laboratory (HWRL) at Oregon State University during fall 2006. The large wave flume is a 104m long, 3.7m wide, and 4.6m deep rectangular concrete channel, and was filled with 611 m^3 of natural beach sand from the Oregon coast with a median grain size of 0.23 mm. The Froude-scaled physical model study (1:6 geometric scale) of dune erosion produced a comprehensive, near prototype-scale data set of hydrodynamics, sediment transport, and morphological evolution during an extreme dune erosion event (see Palmsten and Holman, 2012, for more details on the experiment).

The moveable bed beach/dune system was initially brought to equilibrium with pre-storm random wave conditions in which waves did not reach the toe of the dune and no dune erosion occurred. The physical model was then subjected to attack from steadily increasing water levels and offshore wave heights simulating a natural storm surge hydrograph (Figure 2). During this period of the experiment waves exceeded the dune toe and dune erosion did occur (Palmsten and Holman, 2012). The maximum observed significant wave height (H_s), peak spectral wave period, and storm surge modeled in the flume were 1.3 m, 4.9 s, and 0.17 m respectively. The experiment was carried out in 15 minute increments then the standing wave energy was allowed to settle before the tests continued.

In situ beach profiles were collected using two methods. The subaqueous profile was determined using an acoustic sensor while the subaerial profile was collected using a laser range finder. Profiles were collected every hour throughout the experiment, which lasted 24 hours, and vertical and horizontal resolutions of the profiling system were estimated to be approximately 0.02 m (Palmsten and Holman, 2012).

Application to the Oregon and Washington Coast

The TWL and wave runup formulations, and ultimately the three erosion models, are next applied with field data from the PNW. Utilizing an event selection approach, we examine overtopping and erosion during a major northeast Pacific extratropical cyclone with an approximately 30-year return period that struck the PNW coastline between March 2–4, 1999 (Allan and Komar, 2002). During the storm, observed significant wave heights and peak spectral periods measured at the National Data Buoy Center (NDBC) Columbia River Buoy (Station # 46029) exceeded 12 m and 16 s respectively (Allan and Komar, 2002) (Figure 3). Since the wave buoy is in intermediate water, wave heights were de-shoaled using linear wave theory to obtain the deep-water equivalent wave heights (H_0') for use in wave runup calculations (Eq. 2). Non-tidal residuals (primarily storm surge) of approximately 1.6 m were measured at the National Oceanic and Atmospheric Administration (NOAA) Toke Point, WA Tide Gage (Station # 9440910). These storm conditions are similar to those used to determine coastal erosion hazard zones by the Oregon Department of Geology and Mineral Industries (DOGAMI) (Allan and Priest, 2001) for the state of Oregon. While similar offshore wave conditions were observed at the Newport, OR wave buoy (# 46050, approximately 180 km to the south) the peak non-tidal residual measured at the Yaquina Bay Tide Gauge (# 9435385) was approximately half of that measured at Toke Point (Allan and Komar, 2002). Our goal here is not to resolve alongshore the variability of dune erosion due to alongshore variability in individual storm characteristics – parameters that are typically poorly known. Instead, we are interested in the extent of dune erosion predicted by each model in the event that the maximum storm conditions measured in the region impact all littoral cells directly.

We apply the March 1999 storm conditions to three distinct study areas in the PNW (Figure 1). Long Beach, WA, is the most northern study area and a sub-cell of the Columbia River Littoral Cell (CRLC). It is a large accreting barrier spit that has formed immediately north of the Columbia River mouth. The foredunes in Long Beach are geologically young and relatively low as they continually build out to keep up with a rapidly prograding beach (Ruggiero *et al.*, 2011). The second study site is Clatsop Plains, OR, another sub-cell of the CRLC that is immediately south of the Columbia River mouth. Most of Clatsop Plains consists of relatively tall and wide foredunes that are relatively resistant to erosion and overtopping. However, the southern section of the sub-cell, including the town of Seaside, is particularly vulnerable to erosion as the foredunes are small and provide little protection for buildings and residences. Finally, we examine foredune erosion and overtopping in Rockaway, OR, a littoral cell that is bordered by Tillamook Head to the north and Cape Meares to the south. This study area has several sites with documented erosion issues (Allan and Priest, 2001) and valuable coastal infrastructure is located directly behind the relatively low foredunes.

Extracting Beach and Foredune Morphometrics from Airborne Lidar Data

Beach and foredune geomorphic parameters relevant to foredune erosion were extracted from lidar data collected in September 2002, when the coasts of northern California, Oregon, and Washington were surveyed during the National Aeronautics and Space Administration (NASA)/United States Geological Survey (USGS) Airborne Lidar Assessment of Coastal Erosion (ALACE) Project (NOAA Coastal Services Center, 2002; USGS St. Petersburg Coastal and Marine Science Center, 2002). Airborne topographic lidar surveys have been conducted in many regions to analyze coastal change and vulnerability to storm induced flooding and erosion (*e.g.*, Brock *et al.*, 1999; Brock and Sallenger, 2001; Elko *et al.*, 2002; Sallenger *et al.*, 2003; Shrestha *et al.*, 2005; Stockdon, Doran, and Sallenger, 2009).

Since geomorphic features, such as *dhigh*, are typically easily identifiable on individual cross-shore beach profiles (Figure 4), we developed cross-shore profiles from lidar data that were interpolated on to an evenly spaced grid and filtered to eliminate geospatial noise (Plant, Holland, and Puelo, 2002; Stockdon, Doran, and Sallenger, 2009). Lidar point cloud data were first rotated such that individual gridded surfaces were oriented in the alongshore and cross-shore direction for each stretch of beach. Individual grids consisted of approximately 2 km long sections of data in which the average shoreline orientation was used to rotate the raw data. Gridded surfaces with 2.5 m spacing in the cross-shore direction and 5 m spacing in the alongshore direction minimized vertical interpolation errors, particularly at the dune crests. A quadratic loess filter (Plant, Holland, and Puelo, 2002), with smoothing window sizes of 5 m in the cross-shore direction and 10 m in the alongshore direction, further minimized vertical interpolation errors while preserving the required cross-shore resolution to identify important features.

The geomorphic parameters that are important to coastal dune overtopping and erosion include *dtoe*, the backshore beach slope defined as the average slope between the horizontal location of mean high water (MHW) and *dtoe*, beach width (length from MHW to *dtoe*), *dhigh*, dune heel elevation (*dheel*), and dune width (length from toe to heel) (Figure 4). These features were automatically extracted from all lidar-derived cross-shore profiles with resolved features and morphology (approximately 95% of all profiles) using the approach described below. Unless otherwise noted, all elevations of geomorphic and hydrodynamic parameters are relative to the land based NAVD88 datum.

The 'shoreline' is defined here as the horizontal location of the MHW elevation, taken as 2.1 m NAVD88 following Weber, List, and Morgan's (2005) designation of an operational MHW for coastal change studies. It was determined from a linear regression fit to the elevation data within +/- 0.5 m of MHW following Stockdon *et al.* (2002). The foredune is often identified as the highest elevation on a cross-shore profile for beaches on the U.S. east and Gulf coasts (Stockdon, Doran, and Sallenger, 2009). However, several beaches in the PNW have multiple dune ridges, particularly in prograding areas such as the Long Beach Peninsula in southwest Washington State (Gelfenbaum and Kaminsky, 2010). Here the foredunes can be shorter than geologically older dunes (Psuty, 1992) and cannot be identified with this technique. Cooper (1958) found that foredunes in the PNW typically have a minimum vertical elevation difference of 0.60 m between the dune crest and dune heel and this was verified during multi-year dune surveys as part of the Southwest Washington Coastal Erosion Study (SWCES, Gelfenbaum and Kaminsky, 2010; Ruggiero *et al.*, 2005). Therefore, we identify the foredune on a cross-shore profile as the most seaward profile perturbation (dune) with this distinguishing characteristic.

On each cross-shore profile (Figure 4), *dtoe* is selected automatically by detrending the section of the cross-shore profile between the shoreline and foredune crest with a cubic polynomial and finding the overall minimum on the detrended profile. *dheel* is selected as the minimum elevation between the foredune crest and the next landward local maxima in the profile. To visually check the accuracy of the foredune geomorphic parameters the locations of *dtoe*, *dhigh*, and *dheel* are overlaid on aerial photographs (2005-2010) using GIS and GoogleEarth. Spurious points are either re-selected by hand from each cross-shore profile or removed entirely from future analyses. We calculate the vertical Root Mean Squared Error (RMSE) for *dtoe* and *dhigh* which includes vertical interpolation errors that result from gridding and interpolating the data (Plant, Holland, and Puelo, 2002) and vertical selection errors which result from uncertainty in automatically selecting each feature. The two components of error are combined in quadrature (Taylor, 1997). The selection error is estimated by randomly selecting 30 profiles from each study area, visually indentifying the geomorphic features on these profiles, and comparing these verified features with the features automatically selected by the routines described above.

To estimate interpolation errors in the backshore slope, we divide the vertical interpolation RMSE for *dtoe* by the beach width, and compute the mean for each study area. Errors in the shoreline position (*e.g.*, Stockdon *et al.*, 2002) are relatively small and do not yield significant uncertainty in beach slope calculations. Similar to the procedure for *dtoe* and *dhigh*, the selection error component is estimated by comparing the verified backshore slopes with the automatically extracted slopes. The bias for all features is calculated as the mean difference between the verified features and the automatically selected features.

Foredune Erosion Models

We apply three simple, yet fundamentally different, foredune erosion models and assess them for their appropriateness in estimating foredune erosion along the U.S. west coast. Below we discuss the assumptions inherent in the foredune erosion models and the methodologies used to apply them to three littoral cells in the PNW.

The K99 Geometric Model

The K99 model is a simple conservative geometric foredune erosion model which assumes that the inland erosion distance is a function of the difference between the maximum TWL achieved during a storm and the elevation of the toe of the dune. The retreat distance of the dune toe occurs along the backshore slope as

$$E_{K99} = \frac{(TWL - dtoe)}{tan\beta_b} \quad (3)$$

where E_{K99} is the maximum potential dune toe retreat distance during a storm (Komar *et al.*, 1999). While simple, this model is recommended by the Federal Emergency Management Agency (FEMA) as one approach for estimating erosion during storms for Pacific coast beaches (FEMA, 2005). This approach is also currently used by the State of Oregon in determining coastal hazard zones (Allan and Priest, 2001).

The KD93 Equilibrium Profile Model

The KD93 equilibrium profile foredune erosion model is more complex than K99 and assumes that the volume of sediment eroded from the foredune during storms is deposited in the nearshore as a new equilibrium profile is established (Kriebel and Dean, 1993). The model initially predicts a potential erosion response for a particular storm based upon equilibrium profile theory. Kriebel and Dean (1993) extend this time-independent approach by assuming that beaches and dunes do not erode instantaneously and that the time scale for an erosion response is often greater than a typical storm duration. Therefore, they develop a method to estimate the time scale of the erosion response and the potential erosion is adjusted by the ratio of the two time scales. The maximum potential foredune retreat distance, E_KD93_{∞}, is predicted by

$$E\_KD93_{\infty} = \frac{(TWL - MHW)\left(x_b - \dfrac{h_b}{\tan\beta_f}\right)}{dhigh - MHW + h_b - (TWL - MHW)/2} \quad (4)$$

where x_b is the surf zone width from the MHW position determined using an equilibrium profile (Dean, 1977; Kriebel and Dean, 1993), h_b is the breaking wave water depth relative to MHW, and $\tan\beta_f$ is the foreshore beach slope (Kriebel and Dean, 1993). The relationship is derived geometrically by assuming that sand is conserved as it is eroded from the beach and dune and deposited offshore. We note that Kriebel and Dean (1993) originally developed (Eq. 4) to be applicable to beaches impacted by hurricanes and nor'easter storms when storm surge dominates TWL elevations. To adapt the model to the U.S. west coast, where wave runup is typically a larger component of the TWL than storm surge (Allan and Komar, 2002; Komar *et al.*, 1999; Ruggiero *et al.*, 2001), we use the maximum TWL during a storm rather than just the storm surge to drive the model. The backshore begins to erode when the TWL exceeds MHW. The foreshore slope ($tan\ \beta_f$), estimated as the slope of the profile within +/- 0.5 m vertically of MHW, is used to determine all initial equilibrium profile characteristics while the backshore slope is used when computing wave runup.

To apply the KD93 equilibrium dune erosion model it is necessary to estimate the equilibrium shape parameter, *A*, which is related to median sediment grain size (D_{50}) and describes the concavity of an equilibrium beach profile (Dean, 1977). *A* can be fit to the nearshore portion of a profile or calculated directly from D_{50}. However, our lidar data provide no information from the subaqueous region of the profile or about sediment grain size. Since foreshore beach slope is roughly correlated with sediment grain size (Komar, 1998; Wiegel, 1964) we utilize coincident measurements of foreshore slope (from GPS-derived cross-shore profiles of the nearshore and beach face) and D_{50} that were collected at 44 locations in the CRLC during the summers of 1997, 1998, and 1999 as part of the SWCES (Gelfenbaum and Kaminsky, 2010; Ruggiero *et al.*, 2005). The measurements of foreshore slope and D_{50} are correlated at the 95% level (r = 0.55, not shown). We use the least squares method to fit an equilibrium profile (*e.g.*, Dean, 1977) to each of these profiles below MHW. To develop a predictive equation for *A*, we fit a linear regression between the foreshore slope and best-fit shape parameter at each profile (solid line Figure 5, left panel)

$$A = 0.036 + 2.26(tan\beta_f). \qquad (5)$$

Using (Eq. 5) we estimate values of A directly from foreshore slopes which are readily available from lidar. To check the accuracy of (Eq. 5), we also calculate A from measurements of D_{50} using Moore's (1982) Equation (Figure 5, right panel). The RMSE between the values of A predicted by the linear regression (Eq. 5) and Moore's (1982) Equation is 0.016.

The erosion response to a specific storm with limited duration is determined by the ratio of the erosion response time scale (T_S) to the storm duration (T_D). Theoretically, T_S is dependent upon sediment characteristics and the sediments ability to withstand erosive wave forces (Dean, 1977; Kriebel and Dean, 1993). Kriebel and Dean (1993) suggested a relationship for the erosion response time scale as a function of the breaking wave height (H_b), *dhigh*, and the shape parameter A. Kriebel and Dean (1993) approximate T_D as the duration of elevated water level rise due to storm surge above MSL during an east coast hurricane or nor'easter. In our application to the U.S west coast we consider T_D to be the number hours that TWLs exceed MHW throughout the storm. The ratio of the erosion response time scale and the storm duration, $\alpha = T_D/T_S$, is used to determine the ratio of time-dependent erosion to potential erosion as follows:

$$E_{KD93} = \alpha(E_{KD93\infty}) \tag{6}$$

The L04 Wave Impact Model

Larson, Erikson, and Hanson (2004) developed an analytical wave impact model, L04, to predict the volume eroded from foredunes during a storm. This model is an extension of Overton, Fisher, and Hwang's (1994) model which assumes that the weight of eroded sand is a linear function of the wave impact force

$$W = C_E F; \tag{7}$$

where C_E is an empirical coefficient and F is the wave impact force. The L04 model ignores friction between swash and the beach and assumes that the velocity of a bore traveling up the beach is constant. In its simplest version ($L04_1$), the model ignores temporal variations in tide, storm surge, wave period, and runup such that the volume of eroded sediment is given as

$$V_{L04_1} = 4Cs(R - z_0)^2 \frac{t}{T}; \tag{8}$$

where C_s is an empirical coefficient (includes C_E and other parameters), R and z_0 are the wave runup height and dune toe height respectively above a common static water level, t is the time that the dune face is directly exposed to wave attack, and T is a representative wave period (Larson, Erikson, and Hanson, 2004). The $L04_1$ model can be applied with evolving values of wave runup and dune toe height to predict erosion at discrete time steps as a profile erodes throughout a storm, however this approach requires detailed profile measurements during an erosion event. The model can also be applied with select storm conditions to predict the total erosion for an entire storm event. We apply the model in this way and assume the static water level to be the SWL at the time of maximum TWL, and reference z_0 and R to this elevation. We further assume R to be the value of R_2 at the time of maximum TWL. This application is consistent with our application of the K99 and KD93 models as the maximum TWL drives dune erosion. t is the length of time that the TWL exceeds *dtoe* (when the dune is actively eroding), and T is taken here the mean peak wave period during the time that the TWL exceeds *dtoe*.

Larson, Erikson, and Hanson (2004) present techniques for calibrating the model for a particular site. As mentioned above, no quality pre- and post-storm field data exists within our study sites with which to accurately determine the calibration coefficient, Cs. However, in an application using U.S. east coast field observations of dune erosion from Birkemeier, Savage, and Leffler (1998), Larson, Erikson, and Hanson (2004) suggest a value of $Cs = 1.7 \times 10^{-4}$

(hereafter referred to as *Cs1*). Additionally, Larson, Erikson, and Hanson (2004) present a simple empirical equation to calibrate the model using the ratio of wave height to grain size at a particular site. We used data from the laboratory experiment and calculated a larger value of *Cs* = 1.34 x 10^{-3} (hereafter referred to as *Cs2*). In all applications of the $L04_1$ model, we use both *Cs1* and *Cs2* as a lower and upper bound on the coefficient and erosion predictions. In a later section, we discuss the uncertainty in *Cs* and compare the predictions of the model applied with both coefficients to the observations of dune erosion during the laboratory experiment.

A slightly more sophisticated version of the L04 model ($L04_2$) accounts for changes in the SWL due to surge as a storm progresses. It assumes that surge increases linearly in time and the eroded volume is calculated as

$$V_{L04_2} = 4\frac{Cs}{T}\left((R - z_i)^2 t + a(R - z_i)^2 t^2 + \frac{1}{3}a^2 t^3\right) \tag{9}$$

where *a* is the rate of increase in surge. We calculate *a* as the total increase in surge from the March 1999 storm (approximately 1. 6 m) divided by the storm duration (T_D) at each profile where the model is applied. z_i is assumed to be the initial dune toe height above MHW and *R* is again taken as R_2 at the time of maximum TWL, such that the combined maximum SWL and R_2 equal the maximum TWL used in the previous models.

Since $L04_{1,2}$ computes the volume of eroded foredune material while both K99 and KD93 report horizontal retreat distances, we employ a simple geometric approach to estimate the retreat distance from the $L04_{1,2}$ eroded volumes to allow for model comparison. We simply assume that the dune retreats along a planar slope such that the cross-section of eroded volume forms a parallelogram and that the retreat distance can be estimated from the volume and dune face height as

$$E_{L04_{1,2}} = V_{L04_{1,2}}/(dhigh - dtoe). \tag{10}$$

Table 1 summarizes the input parameters required by each model.

RESULTS

The TWL model and each of the three dune erosion models are applied to both the laboratory experiment and lidar data within three distinct PNW littoral cells to compute foredune overtopping and retreat distances (Figure 1).

Laboratory Experiment

The initial beach profile consisted of a flat bottom immediately shoreward of the wave maker, a relatively planar sand beach intersecting the SWL about 80 m shoreward of the wave maker, a steep backshore, and dune (Figure 6). The initial *dtoe* and *dhigh* elevations were approximately 4.2 m and 5.2 m respectively. During the storm phase of the experiment, the maximum TWL reached approximately 4.9 m. and the dune lost approximately 3.8 m^3/m of sand with the majority of sand moving offshore to form a sandbar at a cross-shore location of 50 m.

The dune toe retreated approximately 5.8 m during the experiment (Table 2). Applying the K99 and KD93 erosion models with the hydrodynamics from the peak of the storm yields predicted retreat distances of 4.5 m and 5.9 m respectively. Using *Cs1*, the $L04_1$ model predicts 3.4 m^3/m of eroded volume. Using Eq. 10 to calculate the retreat distance yields a distance of 3.4 m. Using *Cs2*, the $L04_1$ model predicts 26.8 m^3/m of eroded volume and 26.8 m of retreat.

Application to the Oregon and Washington Coasts

Foredune morphometrics were successfully extracted from cross-shore profiles with a nominal spacing of 5 m in the alongshore. The high resolution foredune morphometrics reveal variability in geomorphology within each study area and on a larger scale highlight the differences between study areas.

Foredune Geomorphology

The extracted parameters along the Long Beach Peninsula are shown in Figure 7 with values smoothed in the alongshore direction over a length scale of 250 m (Plant, Holland, and Puelo, 2002) to reduce noise and small-scale variability. We focus on the backshore slopes, *dhigh*, and *dtoe* elevations as these parameters are used in the estimates of vulnerability to overtopping and erosion. In general, the *dtoe* elevations are similar at all three study areas (Table 3). The *dhigh* elevations are similar at Long Beach and Rockaway while the dunes are taller and more variable in the Clatsop Plains. On average, the backshore is slightly steeper at Rockaway than Long Beach or Clatsop Plains. Foredune morphometrics calculated from the 2002 lidar data for all dune-backed beaches in the PNW (Figure 1) are given in Mull (2011).

The total vertical RMSE values for *dtoe* are greater than those for the other parameters, although they are generally less than 1 m. This is most likely due to the fact that the data was collected after the summer months when wind-blown sand typically fills in and obscures the distinct beach-dune junction making it difficult to identify on a profile. The selection RMSE values are reasonably similar to a comparable technique developed by Elko *et al.* (2002), which resulted in RMSE values of 0.50 m and 0.23 m for the extraction of *dtoe* at two east coast beaches. The mean selection RMSE values for *dhigh* also compare well with Elko *et al.* (2002).

The vertical biases for *dtoe* and *dhigh* are less than the vertical measurement RMSE for the lidar scanner (0.20 m). The RMSE values and biases for the backshore slope are relatively low.

Estimating Overtopping and Erosion

The lidar derived geomorphic parameters enable us to analyze overtopping and erosion at most profiles within each study area for a particular storm event. Maximum TWLs in Long Beach from the March 1999 storm conditions (Figure 7) exceed the *dtoe* elevations at all of the profile locations, indicating that 100% of the profiles would at least be in the Collision Regime of the Sallenger (2000) Storm Impact Scale if the event impinged on the 2002 topography. Maximum TWLs exceed the *dhigh* elevations (Overtopping Regime) at only approximately 10.3% of the cross-shore profiles (Table 4), primarily at the northern and southern ends of the peninsula where dune crest elevations are low. In the Clatsop Plains, maximum TWLs again exceed the *dtoe* elevations at all of the profiles so that they also are at least in the Collision regime of the Sallenger (2000) impact scale. However, only approximately 4.7% of the Clatsop Plains profiles are predicted to be overtopped. All of the overtopped profiles are in the southern section of the littoral cell within the highly developed community of Seaside, OR. Maximum TWLs are also at least in the Collision Regime of the Sallenger (2000) Impact Scale for all of the profiles in Rockaway. Dune overtopping is predicted for approximately 23.5% of the profiles; some of which are located in the developed community of Rockaway Beach, OR.

Similar to the simple application of the storm impact scale, the erosion modeling results suggest that there are sites within all three study areas that are vulnerable to erosion. The K99 model is generally the most conservative model and predicts the largest retreat distances for the three study areas while the $L04_{1,2}$ models are least conservative and predict the smallest retreat distances (Figure 7; Table 4). Profiles with relatively low beach slopes and dune toes, including areas with paths and beach access roads, coincide with spikes in the K99 erosion distance. These areas are clearly susceptible to dune erosion. The $L04_1$ and $L04_2$ models generally predict the same alongshore pattern of erosion at slightly different scales. The KD93 and $L04_{1,2}$ models are not valid for overtopped profiles (Kriebel and Dean, 1993; Larson, Erikson, and Hanson, 2004) and these profiles are excluded from further analysis.

DISCUSSION

Below we test the sensitivities of the TWL calculations and each foredune erosion model to variability in the input geomorphic parameters, we assess the accuracy of the models with the limited data we have available, and finally we develop simple indices to synthesize the regional analyses of overtopping and erosion vulnerability.

Erosion Model Sensitivity

To understand the fundamental differences between the models, they are tested for sensitivity to critical geomorphic input parameters (Table 1) with a range of values equivalent to the total RMSEs of the automatically selected parameters (Table 3). Generally, the models are all sensitive to variations in beach slope while the K99 and $L04_1$ models are sensitive to variations in *dtoe*. The errors and biases for slope are relatively low in all three study areas with a maximum total RMSE in Clatsop Plains of approximately 0.01. Predicted TWLs (Figure 8) vary by approximately 0.50 m per 0.01 units of slope, suggesting that the uncertainty in the backshore slopes could impact estimates of overtopping. If the predicted TWLs from the 2-4 March 199 storm are all increased by 0.50 m, the percentage of overtopped profiles increases from 4.7% to 9.3%. In Long Beach, where the dunes are smaller, this uncertainty would cause the percentage to increase from 10.3% to 20.8%. The total vertical RMSE for the dune crests in

Long Beach is approximately 0.25 m, also leading to uncertainty in the percentage of overtopped profiles. Clearly a single snapshot in time, the 2002 lidar data does not capture temporal variability in any of the geomorphic parameters. As the foredune crests change through time (Ruggiero *et al.*, 2011), the estimated number of overtopped profiles will change accordingly.

The K99 model is dependent upon TWL, backshore beach slope, and *dtoe* elevation (Table 1). Changing the backshore slope can impact the K99 model in two opposing ways. Generally, increasing the backshore slope tends to increase the TWLs but decrease the predicted erosion distances because a steeper slope will not project as far inland (Komar *et al.*, 1999). The erosion distances predicted by the K99 model in these study areas typically decrease with increasing backshore slope (Figure 8). For these *dtoe* elevations, the effect of higher TWLs is less than the effect of minimized landward retreat. However, erosion distance can be positively dependent upon beach slope for the same storm conditions and relatively high dune toes (shown for toe elevations greater than 7.5 m). For these high *dtoe* elevations, the effect of higher TWLs is stronger than the effect of minimized landward retreat. The maximum *dtoe* elevations for Long Beach, Clatsop Plains, and Rockaway are 6.8 m, 9.1 m, and 7.5 m respectively. The model is relatively sensitive to changes in slope and *dtoe* elevation on flat beaches and relatively insensitive to changes in slope and *dtoe* elevation on steep beaches.

The KD93 model is dependent on many parameters (Table 1), but here we focus on the geomorphic parameters, *A*, *dhigh*, and $tan\ \beta_b$, while also testing for sensitivity to the calculated storm duration T_D (Figure 9). For these tests we make the simplifying assumption that the backshore slope and foreshore slope are equal. Figure 9 shows the sensitivity of the potential erosion (E_KD93_∞), fraction of potential erosion (α), and maximum time-dependent erosion (*E_KD93*) to *A* and *dhigh*. When determining the sensitivity of the KD93 model to the shape parameter, the values of *A* were varied while the slope was held constant. While this is not necessarily realistic as *A* is positively correlated with slope (Figure 5), this assumption enables us to directly determine if uncertainties in our estimates of *A* lead to significant variability in predicted dune retreat distances. In general, increasing the shape parameter decreases the surf zone width which subsequently decreases E_KD93_{∞} (Figure 9a). Increasing *A* also decreases the erosion response time scale (T_S) and increases the estimated fraction of potential erosion that occurs during the storm (α) as a larger value of *A* indicates a narrower profile that needs to come into equilibrium. As discussed previously, the RMSE between *A* predicted by Moore's (1982) equation and the prediction based on beach slope (Eq. 5) is 0.016. This magnitude of uncertainty in the shape parameter leads only to a difference of a few meters in the maximum time-dependent erosion distance (*E_KD93*) for a given *dhigh*, indicating that any inaccuracies in Eq. 5 most likely do not significantly impact the final results (Figure 9c). Figure 9d shows that the maximum time-dependent erosion is sensitive to the time duration of the storm. Storm durations are not consistently defined in the literature and choosing a storm duration can often be subjective. Here we estimate storm duration as the time that the TWL exceeds MHW (plus a small vertical bias to account for typical wave setup elevations (Ruggiero and List, 2009)) intuitively as this is the period when backshore beach and foredune erosion would occur. The mean shape parameter for Long Beach is 0.10 $m^{1/3}$. For this shape parameter, changes in storm duration of one hour lead to differences in the maximum time-dependent erosion distance of only approximately 1 m.

The KD93 model is sensitive to changes in *dhigh*. Retreat distances for the mean *dhigh* elevation for Long Beach with a difference of +/- 1 m are shown in Figure 9. A range of 1 m in dune crest elevation yields a difference in maximum time-dependent erosion of a few meters over a range of *A* values. However, changes in the dune crest elevation on the order of total vertical RMSE values for the dune crests (0.20 – 0.40 m) are relatively small, implying that inaccuracies in *dhigh* extracted from the lidar data most likely do not lead to significant variability in computed final erosion distances.

For tests of sensitivity to backshore beach slope, slope is varied and *A* values are calculated from the linear regression between slope and *A* (Eq. 5). Figure 10 shows the sensitivity of the potential erosion (E_KD93_∞), fraction of maximum time-dependent erosion (α), and maximum event-based erosion (*E_KD93*) to the backshore slope and *dhigh*. Varying the slope impacts the maximum event-based erosion distance in two competing ways. In general, as beach slope increases, TWL values increase, *A* values increase, and surf zone width decreases each of which lead to a decrease in E_KD93_∞ (Eq. 5 and Figure 10a). However, a steeper slope also leads to a decrease in the erosion response time scale (T_S) and an increase in α (Figure 10b). Generally speaking, a steeper, narrower profile experiences a more complete erosion response than a flatter, narrower profile as it takes less time to come into equilibrium with storm conditions and erodes more quickly (Kriebel and Dean, 1993). This result creates an upper bound on maximum erosion predictions for extremely steep beaches. The predicted *E_KD93* retreat distances are more sensitive to changes in *dhigh* on steeper beaches (opposite of the dependence of the K99 model on *dtoe*). For most beach slopes, a difference in crest elevation of one meter causes the predicted *E_KD93* retreat distances to vary by a few meters. This is less than the variability of the K99 model where erosion distances differ by tens of meters with changes in *dtoe* for most beach slopes. The KD93 model is more sensitive to changes in slope on flatter beaches (similar to the K99 model). A slope difference of 0.01 yields a difference in retreat distance of approximately 10 m on all but the steepest beaches. Figure 10c shows that

E_KD93_{∞} has a positive dependence on backshore slope, which is the opposite of the K99 model for the typical range of *dtoe* found on PNW beaches.

Even when applied with the larger calibration coefficient (*Cs2*), the $L04_{1,2}$ models are generally the least conservative and predict the smallest amount of erosion in all three study areas. With *Cs1*, the $L04_1$ model predicts retreat distances of 1.3 m, 1 m, and 3 m on average for Long Beach, Clatsop Plains, and Rockaway respectively (Table 4). The C_s values vary approximately by a factor of eight, and as they are linear coefficients, the $L04_1$ model with *Cs2* predicts retreat distances about eight times as large with distances of 10.4 m, 8.9 m, and 23.1 m for the same three study areas respectively. The $L04_2$ model generally predicts less erosion than this as it incorporates a linear increase in storm surge and accounts for water levels that are initially below the peak TWL when the dune is eroding, but not at the maximum rate.

The $L04_{1,2}$ models are directly dependent on the geomorphic parameter *dtoe*, and indirectly dependent on backshore beach slope through calculations of R_2 (Eq. 2). Here we estimate the sensitivity of the simplest Larson model ($L04_1$) to changes in both of these parameters (Figure 11). The model is less sensitive to changes in slope and toe elevation on flatter beaches and more sensitive to changes in these parameters on steep beaches. With the smaller calibration coefficient (*Cs1*), changes in dune toe elevation on the order of 0.50 m are roughly equivalent to differences in erosion distance of approximately 1 m on flat beaches and 5 m on steep beaches. Changes in slope on the order of 0.01 result in differences in erosion distance of approximately 1 m on flat beaches and 5 m on steep beaches. The uncertainty is greater with the larger calibration coefficient (*Cs2*) as changes in dune toe elevation on the order of 0.50 m yield differences in erosion distance of approximately 10 m on flat beaches and 50 m on steep beaches. Changes in slope on the order of 0.01 are approximate to differences in erosion distance of approximately 5 m on flat beaches and 25 m on steep beaches. The model is positively dependent upon beach slope as increasing the slope increases the magnitude of wave runup and ultimately erosion.

We directly compare the dependence of all the models to beach slope in Figure 12. For the range of dune toes in the PNW, the K99 model is negatively dependent upon beach slope while the KD93 and $L04_1$ models are positively dependent upon beach slope. For relatively dissipative beaches ($tan\ \beta_b$ ranges from 0.01 to 0.03), the K99 model is the most conservative, followed by the KD93 model and the $L04_1$ model. This can clearly be seen in the erosion distances for the northern parts of Long Beach, Clatsop Plains, and Rockaway (Figure 7). These are areas of relatively low backshore slopes and the K99 model diverges from the other models and predicts large retreat distances. The K99 model is attractive because it is straightforward to apply and conservative. However, dune-backed beaches in Oregon and Washington are generally flat and dissipative and the K99 model is relatively sensitive to variations in backshore slope and dune toe elevation on these types of beaches. The $L04_1$ model predicts the least amount of erosion on dissipative beaches, regardless of which calibration coefficient is used. The KD93 model is generally consistent and the least sensitive to variations in backshore slope and dune crest elevation for the range of beach slopes in the three study areas. In addition, the KD93 model results are bounded on very steep and flat beaches, where the other models tend to predict extreme retreat distances. This is due to the opposing effects of beach slope in the model for the calculation of the potential erosion (E_KD93_∞) and the fraction of maximum time-dependent erosion (α) as discussed previously.

We conduct variance-based sensitivity tests for the three models with respect to wave height, wave period, and backshore slope (Figure 13). For these tests, we vary wave heights and periods based on characteristics of the 2-4 March 1999 storm, between 10-15 and 15-20 s respectively, and the backshore slope between .01-.10. For each test for sensitivity to a particular parameter, all other parameters all parameters are held constant at representative values for Long Beach (*e.g.*, H_0=12.5 m, T_p=17.5 s, $\tan \beta_b$ = 0.03, *dtoe* = 5 m, and *dhigh* = 10 m). It is interesting to note that the K99 varies approximately on the order of tens of meters with changes in all three parameters. The KD93 model varies approximately on the order of meters with changes in all three parameters. The $L04_1$ model varies approximately on the order of meters with changes in the wave parameters and on the order of tens of meters with variations in backshore slope. All models are more sensitive to changes in backshore slope than the wave parameters indicating that variations in slope have a larger impact on predicted erosion distances than variations in the wave forcing. The KD93 model is the least sensitive to backshore slope further indicating that the model predictions are bounded for very flat and steep beaches.

Accuracy of Dune Erosion Models

While there are no direct observations available from the 2-4 March 1999 storm with which to compare to model results, Allan and Priest (2001) and Allan and Komar (2002) qualitatively report that foredune retreat distances on the order of tens of meters occurred in Rockaway, OR during the storm. This suggests that the estimated retreat distances predicted by all three models are at least reasonable. Foredunes in southwest Washington were observed to have experienced some overtopping and some coastal roads were flooded during the event, an observation supported by our TWL calculations. Foredunes throughout northwest Oregon and southwest Washington were severely scarped during this event (Jonathan Allan and George Kaminsky, personal communication), suggesting that the majority of dunes were in the collision regime of the Sallenger (2000) storm impact scale. There were no reports of foredunes completely eroding during the storm, indicating that the K99 model, which predicts that 100% and 91% of the foredunes in Long Beach and Rockaway respectively will completely erode, may be overly conservative.

Both the K99 and KD93 models predict reasonable retreat distances compared to the observed retreat during the 2006 dune erosion experiment (Figure 6). Using *Cs1*, the $L04_1$ model predicts an eroded volume which is close to the observed eroded volume. Using Eq. 10 to calculate the retreat distance under-predicts the retreat distance by approximately 41%. Using *Cs2*, the $L04_1$ model over-predicts erosion. It is important to note that Palmsten and Holman (2012) found accurate results when applying the $L04_1$ model with C_s2 in hourly time steps to the same experiment data. However, when the model is applied in discrete time steps, it can account for geomorphological feedbacks such as the retreat of the dune toe up the beach which decreases subsequent wave collisions and erosion from the dune face (Larson, Erikson, and Hanson, 2004; Palmsten and Holman, 2012). These results suggest that *Cs2* is too large when applying the model once with a single set of storm conditions and that an appropriate value of *Cs* is between *Cs1* and *Cs2*. To accurately produce the retreat distance of 5.8 m requires a *Cs* value equal to 2.98×10^{-4}. While this value is 70% larger than *Cs1*, if used with the $L04_{1,2}$ models in the three study areas the wave impact model would still be the least conservative and generally predict the least amount of erosion.

The backshore beach slope in the experiment was steeper (initial $\tan \beta_b = 0.14$) than the typical dissipative dune-backed beach found within the three study areas (Table 3). The K99 model predicts a relatively accurate retreat distance for this experiment, however, as discussed earlier the K99 model is perhaps too conservative for the relatively flat beaches of the PNW and predicts unrealistically large retreat distances. The KD93 model predicts the most accurate retreat distance for this experiment

Synthesizing Vulnerability to Overtopping and Erosion

To synthesize the vulnerability to overtopping of each individual profile, and to compare relative vulnerability between study areas, we normalize the amount of overtopping by the dune face height to create an overtopping index as follows:

$$I_O = \frac{TWL - dhigh}{dhigh - dtoe} \quad (11)$$

Positive values of I_o indicate overtopping and negative values indicate that no overtopping occurred. A value of one indicates that the TWL exceeds *dhigh* by approximately one dune height. While there are many uncertainties in the calculations of TWLs, normalizing the amount of overtopping by the dune height decreases the emphasis on absolute TWL values. The overtopping index for the 2-4 March 1999 storm identifies areas within littoral cells that are particularly vulnerable to overtopping (Figure 14). For example, the index suggests that there is a relatively high vulnerability to overtopping in the southern portion of Clatsop Plains and at Rockaway Beach in the middle of the Rockaway littoral cell. These areas are developed with significant infrastructure directly behind the foredunes which would be immediately impacted by overtopping. An index that is close to zero, but still negative, indicates that a profile will not be overtopped for these storm conditions but may be overtopped during a more extreme design storm (*i.e.*, a storm with a 100-yr return period rather than a 30-yr return period).

The relative vulnerability to overtopping between study areas is compared via regional mean overtopping indices (Table 4). The mean indices are more informative than the percent of overtopped profiles as they provide information about *how much* the TWL values exceed the dune crest elevations. In addition, they can help us assess vulnerability in a regional sense and help us identify which beaches are more exposed to overtopping during a severe coastal storm. The mean overtopping indices indicate that overall Rockaway is the most vulnerable littoral cell to overtopping and that Clatsop Plains is the least vulnerable to overtopping.

To estimate relative vulnerability to erosion we normalize the amount of erosion predicted by each of the dune erosion models by the dune width to create an erosion index for each profile

$$I_E = \frac{E_{max}}{W} \quad (12)$$

where E_{max} is the maximum dune retreat distance predicted by each model and W is the foredune width (Figure 14). The erosion index conveys *how much* of each foredune is eroded and indicates if the foredune, the first line of defense during a severe storm, could be completely eroded away. A value equal to zero indicates no erosion, while a value of one indicates that a particular foredune is predicted to be completely eroded. Values greater than one indicate erosion distances in equivalent dune widths. The index generally indicates a high degree of erosion vulnerability in the PNW even though in general very little overtopping is predicted for this study area.

On average, the erosion models predict that only 3% of the foredunes in the Clatsop Plains could be completely eroded by the design storm event. By comparison, the models predict that on average 30% of the foredunes could be completely eroded in the Rockaway littoral cell by the event of record. The mean erosion indices and percentages of completely eroded foredunes enable us to quickly compare the relative vulnerabilities to erosion between each study area. Both the percentages and the overall mean indices imply that Rockaway is the most vulnerable to erosion while Clatsop Plains is the least vulnerable to erosion. Areas such as

Rockaway, where all of the models predict high vulnerability are most likely truly susceptible to erosion. In fact, dune erosion is a recognized problem in this area and certain sections of the foredunes are actively being armored to slow erosion. In other applications, the erosion index can help identify vulnerable areas before property is threatened and facilitate coastal management decisions such as whether a site should be armored or perhaps left undeveloped.

CONCLUSIONS

Three dune erosion models including a geometric model (K99), an equilibrium profile model (KD93), and a wave impact model ($L04_{1,2}$), have been assessed for applicability to U.S. West coast regional scale coastal vulnerability analyses. Sensitivity tests demonstrate that the K99 model has a negative dependence on beach slope (for typical dune toe elevations in the PNW) while the KD93 and $L04_1$ models have a positive dependence on beach slope. The $L04_1$ model is generally the least conservative (*i.e.*, predicts the greatest retreat distances) while the K99 model is perhaps overly conservative (*i.e.*, predicts the smallest retreat distances) on the relatively flat dissipative beaches that are typical of the PNW. The KD93 model most accurately predicts the foredune retreat distance in a large-scale wave tank experiment. In addition, the estimates of retreat distances for this model are bounded for low and high beach slopes. While the $L04_{1,2}$ models are least sensitive to uncertainties and variability in morphometric input parameters, the approach requires a calibration coefficient that ranges almost over an order of magnitude. Because of these findings, we recommend that of the three simple models tested in this study, the KD93 model is the most applicable for estimating vulnerability to foredune erosion in the PNW.

ACKNOWLEDGEMENTS

Support for this project was provided by grants from the U.S. Environmental Protection Agency (EPA/NCER 83383601-0) and Oregon Sea Grant (NA10OAR4170010). The authors wish to thank Kara Doran and Hilary Stockdon of the USGS St. Petersburg Coastal and Marine Science Center for sharing lidar data, ideas, and technical support. In addition we gratefully acknowledge the help and support of Eric Seabloom, Sally Hacker, and Phoebe Zarnetske who significantly contributed to this project.

LITERATURE CITED

Allan, J.C. and Komar, P.D., 2002. Extreme storms on the Pacific Northwest coast during the 1997-98 El Niño and 1998 La Niña. *Journal of Coastal Research*, 18(1), 175-193.

Allan, J.C. and Priest, G.R., 2001. *Evaluation of Coastal Erosion Hazard Zones Along Dune and Bluff Backed Shorelines in Tillamook County Oregon: Cascade Head to Cape Falcon.* Portland, Oregon: State of Oregon Department of Geology and Mineral Industries, *Open File Report O-01-03*, 126p.

Birkemeier, W.A.; Savage, R.J., and Leffler, M.W., 1998. *A Collection of Storm Erosion Field Data*. Vicksburg, Mississippi: Coastal Engineering Research Center, U.S. Army Engineer Waterways Experiment Station, *Miscellaneous Paper CERC-88-9*, 285p.

Brock, J.; Sallenger, A.H.; Krabill, W.; Swift, R.; Manizade, S.; Meredith, A.; Jensen, M., and Eslinger, D., 1999. Aircraft laser altimetry for coastal processes studies. *4th International Symposium on Coastal Engineering and Science of Coastal Sediment Processes* (Long Island, NY, ASCE), pp. 2414-2428.

Brock, J. and Sallenger, A.H., 2001. *Airborne Topographic Lidar Mapping for Coastal Science and Resource Management.* St. Petersburg, Florida: U.S. Geological Survey, *Open File Report 01-46*, 6p.

Bromirski, P.D.; Flick, R.E., and Cayan, D.R., 2003. Storminess variability along the California coast: 1858-2000. *Journal of Climate*, 16(6), 982-993.

Cooper, W.S., 1958. Coastal Sand Dunes of Oregon and Washington. *Memoirs of the Geological Society of America* (Boulder, Colorado). Memoir 72, pp. 1-6.

Cox, J.C., and Machemel, J., 1986.Overland bore propagation due to an overtopping wave. *Journal of Waterway, Port, Coastal, and Ocean Engineering*, 112(1), 161-163.

Dean, R.G., 1977. *Equilibrium beach profiles: U.S. Atlantic and Gulf Coasts*. Newark, Delaware: University of Delaware, Department of Civil Engineering, *Ocean Engineering Report No. 12*, 45p.

Elko, N.; Sallenger, A.H.; Guy, K.; Stockdon, H., and Morgan, K., 2002. *Barrier island elevations relevant to potential storm impacts: 1. Techniques*. St. Petersburg, Florida: U.S. Geological Survey, *Open File Report 02-287*, 6p.

FEMA, 2005.*Guidelines and Specifications for Flood Hazard Mapping Partners, Section D.4 – Coastal Flooding Analyses and Mapping: Pacific Coast*. Oakland, California: *Technical Report*, 344p.

Gelfenbaum, G., and Kaminsky, G.M., 2010. Large-scale coastal change in the Columbia River littoral cell: An overview. *Marine Geology*, 273(1), 1-10.

Hacker S.D.; Zarnetske, P.; Seabloom, E.; Ruggiero, P.; Mull, J.; Gerrity, S., and Jones, C., 2012. Subtle differences in two non-native congeneric beach grasses significantly affect their colonization, spread, and impact. *Oikos*, 121(1), 138-148.

Holman, R.A., 1986. Extreme value statistics for wave run-up on a natural beach. *Coastal Engineering*, 9(6), 527-544.

Komar, P., 1998. *Beach Processes and Sedimentation*. Upper Saddle River, New York: Prentice Hall Inc., 544p.

Komar, P.; McDougal, W.G.; Marra, J.J., and Ruggiero, P., 1999. The rational analysis of setback distances: Applications to the Oregon Coast. *Shore and Beach*, 67(1), 41-49.

Kriebel, D.L. and Dean, R.G., 1993. Convolution method for time-dependent beach-profile response. *Journal of Waterway, Port, and Coastal Engineering*, 119(2), 204-226.

Larson, M.; Erikson, L., and Hanson, H., 2004. An analytical model to predict dune erosion due to wave impact. *Coastal Engineering*, 51(8), 675-696.

Moore, B.D., 1982. Beach profile evolution in response to changes in water level and wave height. Newark, Delaware: University of Delaware Master's Thesis, p.

NOAA Coastal Services Center. http://ww.csc.noaa.gov/ldart.

Overton, M.F.; Fisher, J.F., and Hwang, K.N., 1994. Development of a dune erosion model using SUPERTANK data. *Proceedings of the 24th International Conference on Coastal Engineering* (Kobe, Japan, ASCE), pp. 2488-2502.

Palmsten, M.L., and Holman, R.A., 2012. Laboratory investigation of dune erosion using stereo video. *Coastal Engineering*, 60(1), 123-135.

Plant, N.G.; Holland, K.T., and Puelo, J.A., 2002. Analysis of the scale of errors in nearshore bathymetric data. *Marine Geology*, 191(1), 71-86.

Psuty, N.P., 1992. Spatial variation in coastal foredune development. *Proceedings of the 3rd European Dune Congress* (Balkema, Rotterdam), pp. 3-13.

Roelvink, D.; Reniers, A.; van Dongeren, A.; van Thiel de Vries, J.; Lescinski, J., and Walstra, D.J., 2007. XBeach Annual Report and Model Description. Delft, Netherlands: Delft University of Technology. *Technical Report,* 45p.

Ruggiero, P.; Komar, P.D.; McDougal, W.G.; Marra, J.J., and Beach, R.A., 2001. Wave runup, extreme water levels, and the erosion of properties backing beaches. *Journal of Coastal Research*, 17(2), 407-419.

Ruggiero, P.; Kaminsky, G.M.; Gelfenbaum, G., and Voight, B., 2005. Seasonal to interannual morphodynamics along a high-energy dissipative littoral cell. *Journal of Coastal Research*, 21(3), 553-578.

Ruggiero, P. and List, J.H., 2009. Improving accuracy and statistical reliability of shoreline position and change rate estimates. *Journal of Coastal Research*, 25(5), 1069-1081.

Ruggiero, P.; Mull, J.; Zarnetske, P.; Hacker, S., and Seabloom, E., 2011. Interannual to decadal foredune evolution. *Proceedings of Coastal Sediments* (Miami, FL), 698-710.

Sallenger, A.H., 2000. Storm impact scale for barrier islands. *Journal of Coastal Research*, 16(3), 890-895.

Sallenger, A.H.; Krabill, W.B.; Swift, R.N.; Brock, J.C.; List, J.H.; Hansen, M.; Holman, R.A.; Manizade, S.S.; Sonntag, J.G.; Merideth, A.; Morgan, K.; Yunkel, J.K.; Frederick, E.B., and Stockdon, H., 2003. Evaluation of airborne topographic lidar for quantifying beach change. *Journal of Coastal Research*, 19(1), 125-133.

Seabloom, E.W.; Ruggiero, P.; Hacker, S.; Mull, J., and Zarnetske, P., 2013. Invasive grasses, climate change, and exposure to storm wave overtopping in coastal dune ecosystems. *Global Change Biology*, 19(3), 824-832.

Shrestha, R.L.; Carter, W.E.; Sartori, M.; Luzman, B.J., and Slatton, K.C., 2005. Airborne laser swath mapping: Quantifying changes in sandy beaches over time scales of weeks to years. *Journal of Photogrammetry & Remote Sensing*, 59(1), 222-232.

Stockdon, H.F.; Sallenger, A.H.; List, J.H., and Holman, R.A., 2002. Estimation of shoreline position and change using airborne topographic lidar data. *Journal of Coastal Research*, 18(3), 502–513.

Stockdon, H.F.; Holman, R.A.; Howd, P.A., and Sallenger, A.H., 2006. Empirical parameterization of setup, swash, and runup. *Coastal Engineering*, 53(7), 573-588.

Stockdon, H.F.; Sallenger, A.H.; Holman, R.A., and Howd, P.A., 2007. A simple model for the spatially-variable coastal response to hurricanes. *Marine Geology*, 238(1), 1-20.

Stockdon, H.F.; Doran, K.S., and Sallenger, A.H., 2009. Extraction of Lidar-based dune crest elevations for use in examining the vulnerability to beaches during inundation during hurricanes. *Journal of Coastal Research*, Special Issue No. 53, 59-65.

Taylor, J.R., 1997. *An Introduction to Error Analysis, the Study of Uncertainties in Physical Measurements*. Sausalito, California: University Science Books, 327p.

USGS St. Petersburg Coastal and Marine Science Center, 2002. http://coastal.er.usgs.gov/lidar.

Weber, K.M.; List, J.H., and Morgan, K.L.M., 2005. *An operational mean high water datum for determination of shoreline position from topographic lidar data*. Woods Hole, Massachusetts: U.S. Geological Survey, *Open-File Report 2005-1027*, 10p.

Wiegel, R.L., 1964. *Oceanographic Engineering*. Upper Saddle River, New York: Prentice Hall Inc., 532p.

TABLES

Table 1: The parameters required for the TWL, K99, KD93, and L04 models.

Model	**Parameters**
TWL	H_0, T_p, $tan\ \beta_b$, η, η'
K99	TWL, *dtoe*, $tan\ \beta_b$
KD93	TWL, $A^{\dagger}$, $tan\ \beta_b$, $tan\ \beta_f$, *dhigh*, *dtoe* H_0, T_p
L04	R_2, η', *dtoe*, *t*, *T*, *Cs**

*Indicates empirical coefficient
†Indicates parameterized variable calculated by best-fit procedure to data

Table 2: Accuracy of Dune Erosion Models in the Laboratory Experiment

Model	Retreat (m)
K99	4.5
KD93	5.9
$L04_1$ (*Cs1*)	3.4
$L04_1$ (*Cs2*)	26.8
Observed	**5.8**

Table 3: Summary Statistics and Vertical RMSE Values for Geomorphic Parameters from the Three Study Areas.

		Long Beach	Clatsop Plains	Rockaway
Dune Toe	Mean (m)	5.46	5.07	5.17
	Standard Deviation (m)	0.55	0.64	0.80
	Selection RMSE (m)	0.47	0.92	0.80
	Interpolation RMSE (m)	0.19	0.21	0.27
	Total RMSE (m)	0.51	0.94	0.84
	Vertical Bias (m)	0.19	-0.05	0.06
Dune Crest	Mean (m)	8.09	13.12	8.44
	Standard Deviation (m)	0.72	2.49	1.73
	Selection RMSE (m)	0.02	0.03	0.04
	Interpolation RMSE (m)	0.25	0.20	0.40
	Total RMSE (m)	0.25	0.20	0.40
	Vertical Bias (m)	<0.01	<0.01	<0.01
Backshore Slope	Mean	0.03	0.03	0.04
	Standard Deviation	0.01	0.01	0.01
	Selection RMSE	<0.01	0.01	<0.01
	Interpolation RMSE	<0.01	<0.01	<0.01
	Total RMSE	<0.01	0.01	<0.01
	Bias	<0.01	<0.01	<0.01

Table 4: Percentage of Overtopped and Completely Eroded Foredunes and Mean Flooding and Erosion Indices for Long Beach, WA, Clatsop Plains, OR, and Rockaway, OR.

Overtopping	**Long Beach**			**Clatsop Plains**			**Rockaway**		
% Overtop	10.3 %			4.7%			23.5%		
Mean I_O	-0.3			-0.6			-0.2		
Erosion									
Model	Mean Retreat (m)	% Eroded	Mean I_E	Mean Retreat (m)	% Eroded	Mean I_E	Mean Retreat (m)	% Eroded	Mean I_E
K99	71	99	1.7	74	20	0.8	72	91	2.4
KD93	33	13	0.8	24	0	0.3	43	62	1.4
$L04_1$ (*Cs1*)	1.3	0	<0.1	1	0	<0.1	3	0	0.1
$L04_2$ (*Cs1*)	<1	0	<0.1	<1	0	<0.1	1	0	<0.1
$L04_1$ (*Cs2*)	10.4	1.9	0.3	8.9	0	<0.1	23.1	24	0.8
$L04_2$ (*Cs2*)	1.1	0	<0.1	1.5	0	<0.1	5.4	0.2	0.2
Overall Average	**20**	**19**	**0.5**	**18**	**3**	**0.3**	**25**	**30**	**0.8**

FIGURE CAPTIONS

Figure 1. Map of the dune-backed beaches in the PNW (shown in red) including the three labeled study areas. Long Beach, WA is a large barrier sand spit north of the Columbia River mouth with relatively small foredunes. Clatsop Plains, OR is a beach with relatively large foredunes south of the Columbia River mouth. Rockaway, OR is a distinct littoral cell with documented issues of dune overtopping and erosion. NDBC buoys are shown in green.

Figure 2. Wave characteristics and initial profile feature elevations from the dune erosion tank experiment. H_s (blue line), T_p (turquoise line), SWL (black line), calculated R_2 (purple line), and calculated TWL (black asterisks) are shown for time steps throughout the experiment. The initial *dhigh* (blue dashed lines) and *dtoe* (red dashed lines) elevations are also plotted.

Figure 3. Storm conditions from the PNW 'storm of record' on March 2–4, 1999. The black line with asterisks is the significant wave height observed at the NDBC Columbia River Buoy (Station # 46029). The solid black line is the peak spectral period measured at the buoy. The black line with dots is the measured tide at the NOAA Toke Point, WA Tide Gage (Station # 9440910). The black dashed line is the predicted tide for this station. The difference between the predicted and measured tides is the non-tidal residual, most of which is attributed to storm surge (Allan and Komar, 2002).

Figure 4. An example of a lidar-derived cross-shore profile and the beach and foredune geomorphic parameters extracted from the profile. The data have been smoothed and interpolated onto a 2.5 m spaced grid in the cross-shore direction. The dhigh elevation indicates

the foredune crest and is the most shoreward dune crest with a minimum backshore drop of 0.60 m. The dune heel (*dheel*) is the lowest swale between dhigh and a subsequent dune crest. The dune toe (*dtoe*) is the maximum difference between the profile and the profile detrended with a cubic function. The dune volume is the numerically integrated area between the profile and the horizontal line at the dtoe elevation. The area can be integrated from the dtoe location to the dheel location for a large estimate of dune volume (*V1*) or from the dtoe location to the dtoe location for a small estimate of volume (*V2*).

Figure 5. The left panel shows a linear regression (black line) between the foreshore slope and best-fit shape parameter for summer profiles within the CRLC. The regression is significant at the 95% confidence level and confidence bands are shown as dashed lines. The right panel shows the values of *A* predicted by the linear regression (Eq. 5) with foreshore slope values from summer profiles within the CRLC as a black line. The values of *A* predicted by Moore's (1982) equation with D_{50} from each summer profile, plotted against the foreshore slopes at each profile. The RMSE between the *A* values is 0.016.

Figure 6. Cross-shore profiles from the dune erosion experiment in the wave flume at the O.H. Hinsdale Wave Laboratory. The initial profile, final profile, observed retreat distance, and predicted retreat distances by each model are indicated. The KD93 model most accurately predicts the observed retreat distance.

Figure 7. Foredune parameters, overtopping, and erosion for the three study areas. The left panel indicates the alongshore position of each profile. The next panel shows backshore slopes in dark grey and backshore slopes that have been smoothed in the alongshore direction (red). The next panel shows dtoe elevations in light grey and dhigh elevations in dark grey with both parameters smoothed in the alongshore (red and blue respectively). Smoothed TWL elevations are shown in green. The right panel shows the smoothed dune retreat distances predicted by the K99 model (red) the KD93 model (blue), the $L04_1$ model with *Cs1* (purple), the $L04_2$ with *Cs1* model (turquoise), the $L04_1$ model with *Cs2* (dashed purple), and the $L04_2$ with *Cs2* model (dashed turquoise).

Figure 8. Dependence of the TWL and K99 model on backshore beach slope. The left panel shows the TWL values for different slopes with the maximum wave height, period, and surge from the storm of record. The right panel shows dune retreat distances predicted by the K99 model with a range of slopes and three dune toe elevations: the mean *dtoe* for Long Beach (5.5 m) and the mean plus and minus the total dune toe RMSE (0.5 m) for Long Beach. Retreat distances for the high *dtoe* of 7.5 m are plotted to illustrate that the model switches to a positive dependence on beach slope for higher dune toes.

Figure 9. Dependence of A) the potential erosion (E_KD93_∞) on the shape parameter and foredune crest elevation; B) fraction of potential erosion (α) on the shape parameter and foredune crest elevation; C) maximum time-independent erosion (*E_KD93*) on the shape parameter and foredune crest elevation with a storm duration of six hours; and D) maximum time-dependent

erosion (*E_KD93*) on the shape parameter and total storm duration (T_D). dhigh elevations of 7 m, 8 m, and 9 m are shown in blue, green, and red respectively.

Figure 10. Dependence of A) the potential erosion (E_KD93_∞) on the backshore slope and foredune crest elevation; B) fraction of maximum time-independent erosion (α) on the backshore slope and foredune crest elevation; and C) maximum time-dependent erosion (*E_KD93*) on the backshore slope and foredune crest elevation with T_D ranging from 30 – 40 hrs.

Figure 11. Dependence of eroded volume (left panel) and retreat distance (right panel) predicted by the $L04_1$ model on dtoe and backshore slope. Three dune toe elevations are tested: the mean dtoe for Long Beach (5.5 m) and the mean plus and minus the total dune toe RMSE (0.5 m) for Long Beach. To calculate retreat distance, the mean dhigh elevation for Long Beach (8 m) is used.

Figure 12. Dependence of the K99 (solid lines), KD93 (dashed lines), $L04_1$ with *Cs1* (bold dashed lines), and $L04_1$ with *Cs2* (dashed lines) models on beach slope. For the K99 and $L04_1$ models, dtoe elevations of 5 m, 5.5 m, and 6 m are shown in blue, green, and red respectively. For the KD93 model, dhigh elevations of 7 m, 8 m, and 9 m are shown in blue, green, and red respectively.

Figure 13. Variance-based sensitivity tests of the three erosion models with respect to wave height, wave period, and backshore slope. The K99 varies approximately on the order of tens of meters with changes in these parameters. The KD93 model varies approximately on the order of

meters with changes in these parameters. The $L04_1$ model varies approximately on the order of meters with changes in the wave parameters and on the order of tens of meters with variations in backshore slope. All models are most sensitive to changes in backshore slope.

Figure 14. Smoothed overtopping and erosion indices for Long Beach, Clatsop Plains, and Rockaway. The overtopping index normalizes the amount of overtopping by the height of the foredune to give relative vulnerability of overtopping. The erosion index normalizes the amount of erosion by the foredune width. The right panel shows the smoothed erosion indices predicted by the K99 model (red) the KD93 model (blue), the $L04_1$ model with *Cs1* (purple), the $L04_2$ with *Cs1* model (turquoise), the $L04_1$ model with *Cs2* (dashed purple), and the $L04_2$ with *Cs2* model (dashed turquoise).

Figure
Click here to download high resolution image

Figure

Click here to download high resolution image

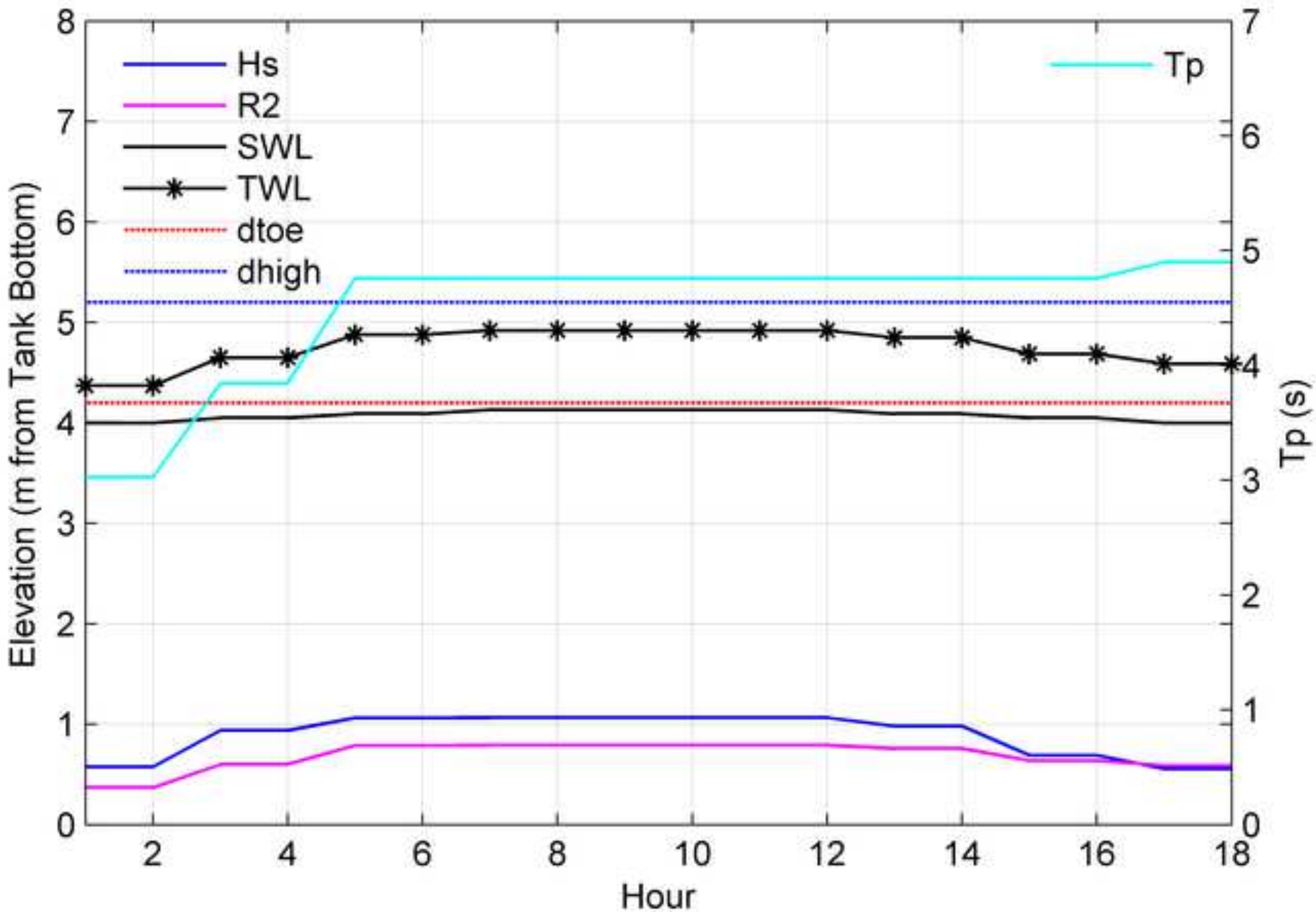

Figure
Click here to download high resolution image

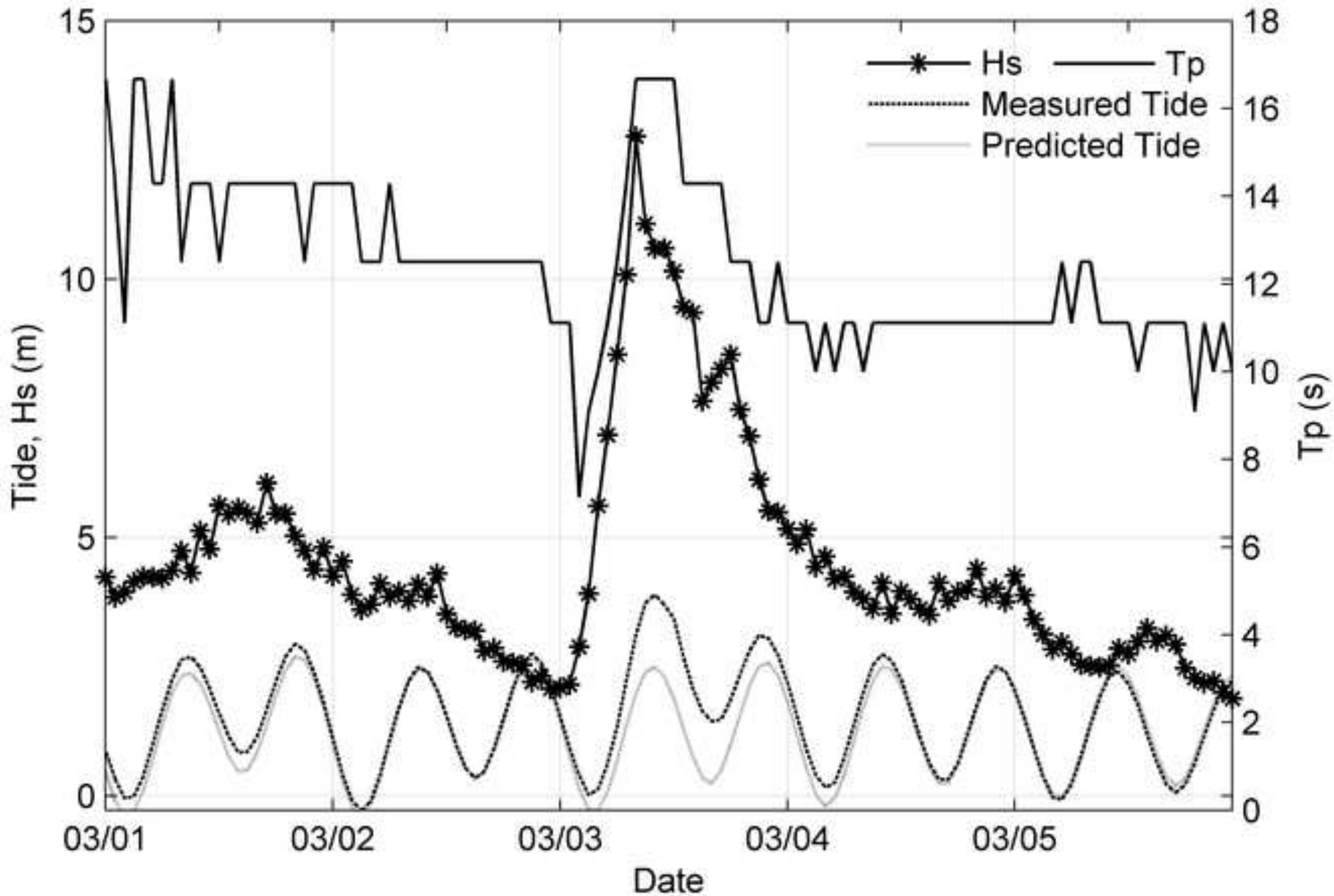

Figure
Click here to download high resolution image

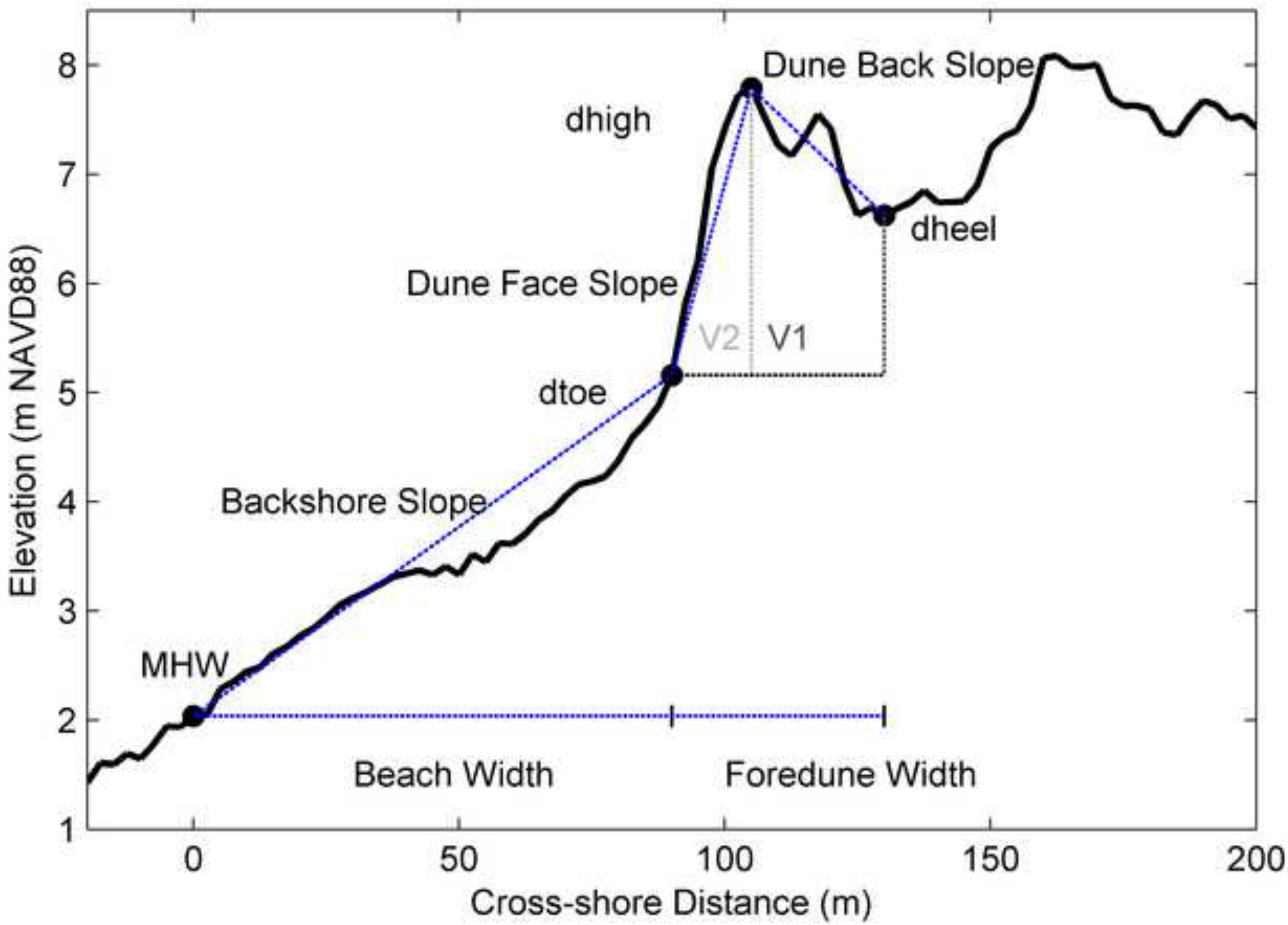

Figure
Click here to download high resolution image

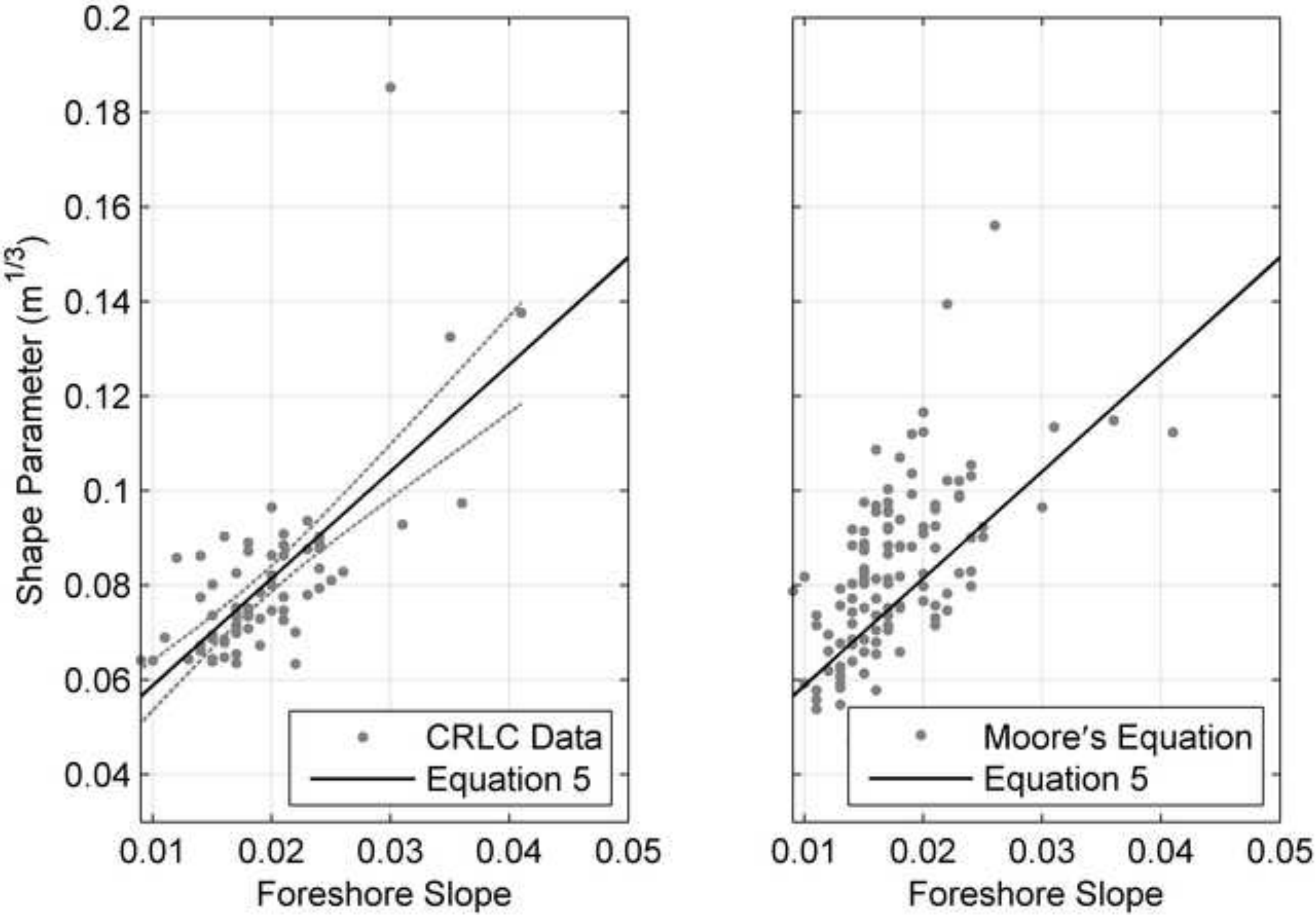

Figure
Click here to download high resolution image

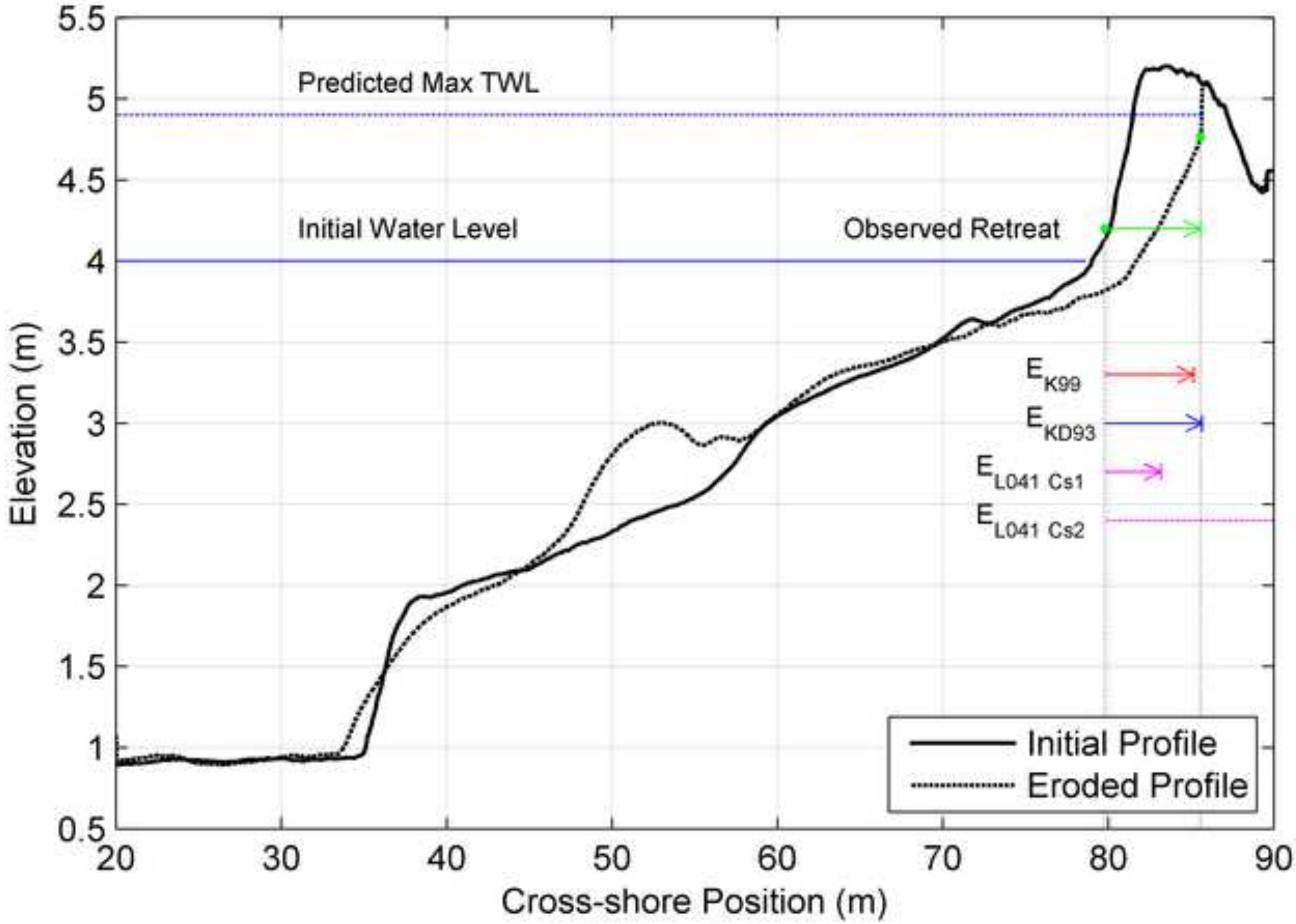

Figure
Click here to download high resolution image

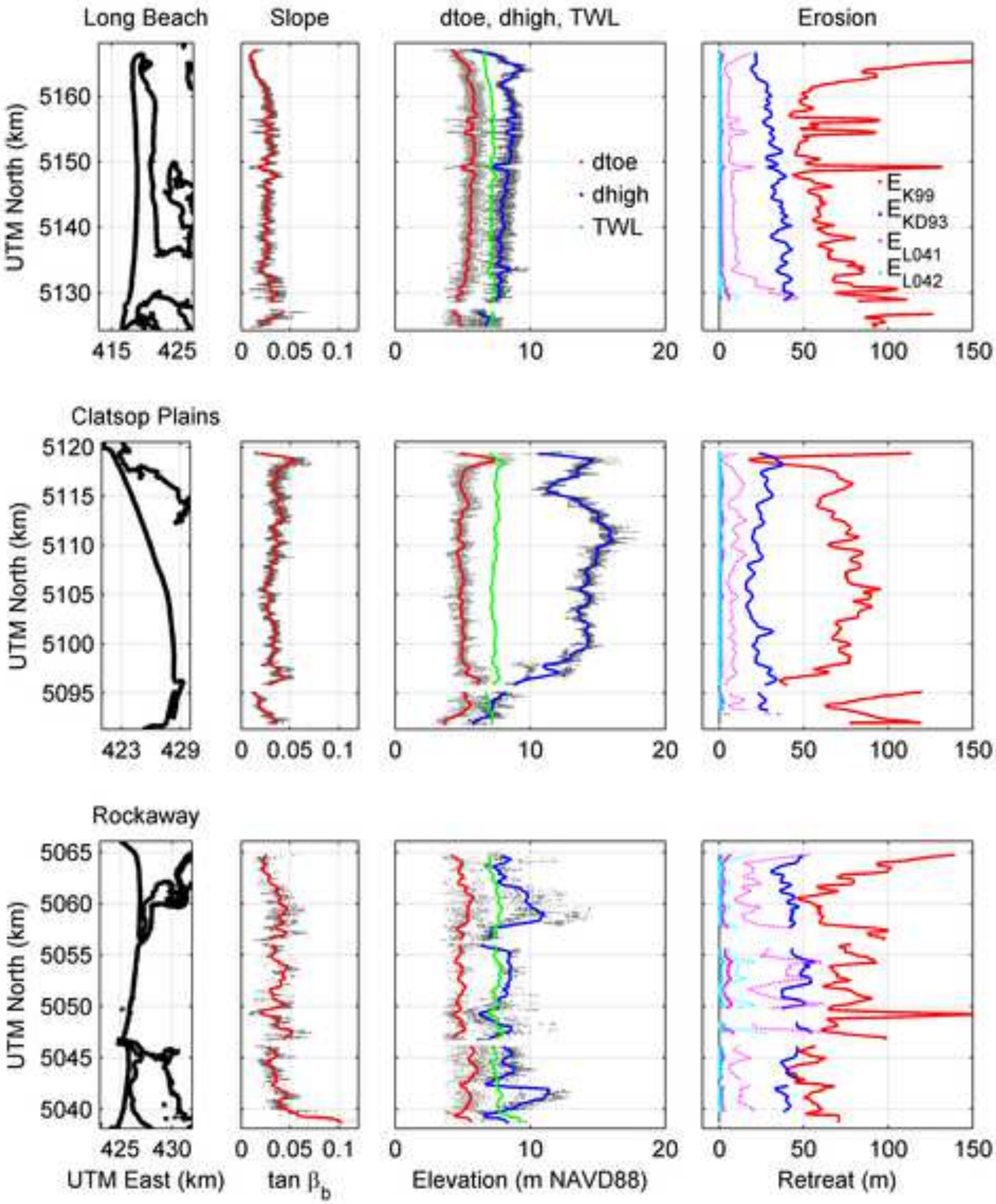

Figure
Click here to download high resolution image

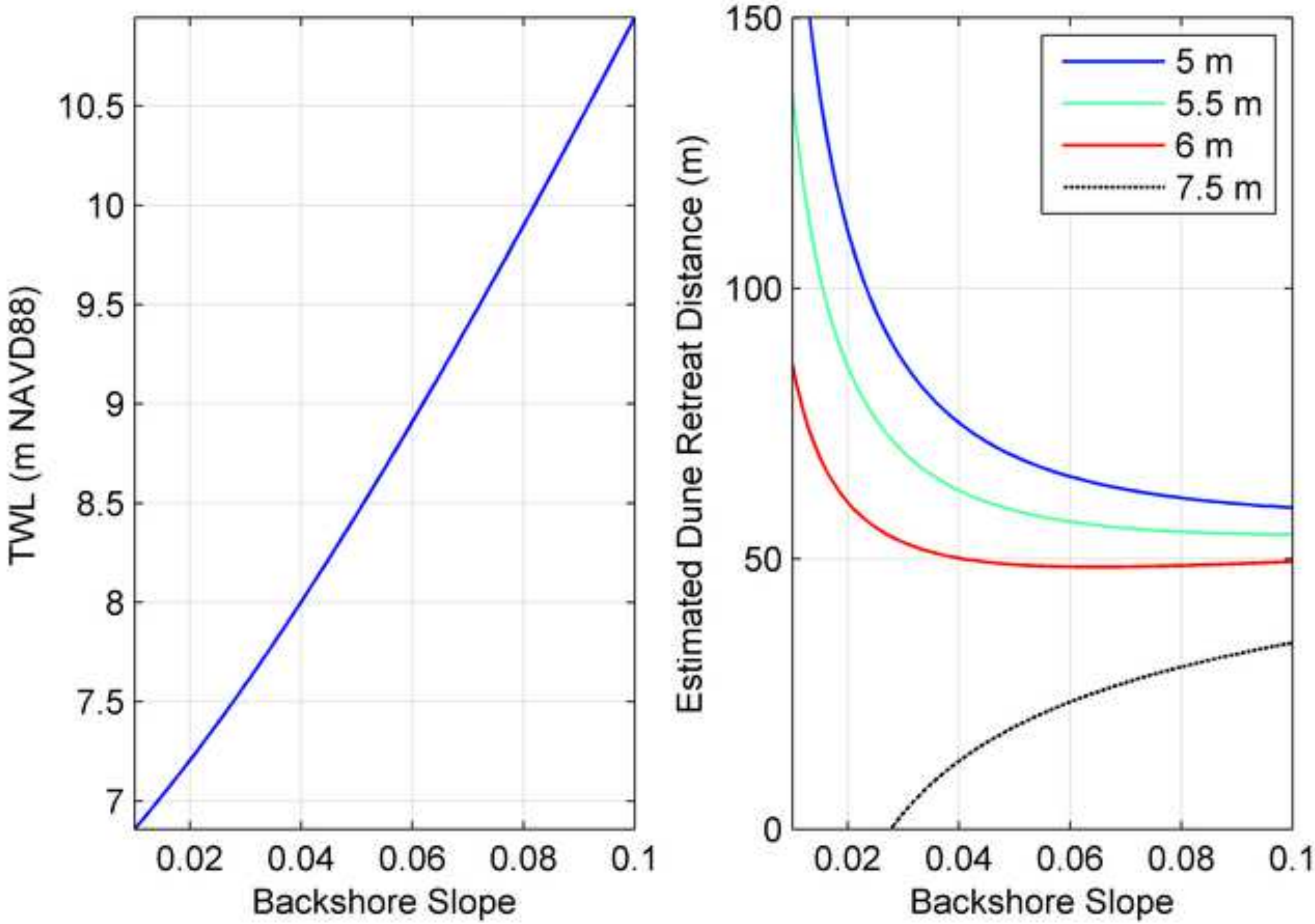

Figure

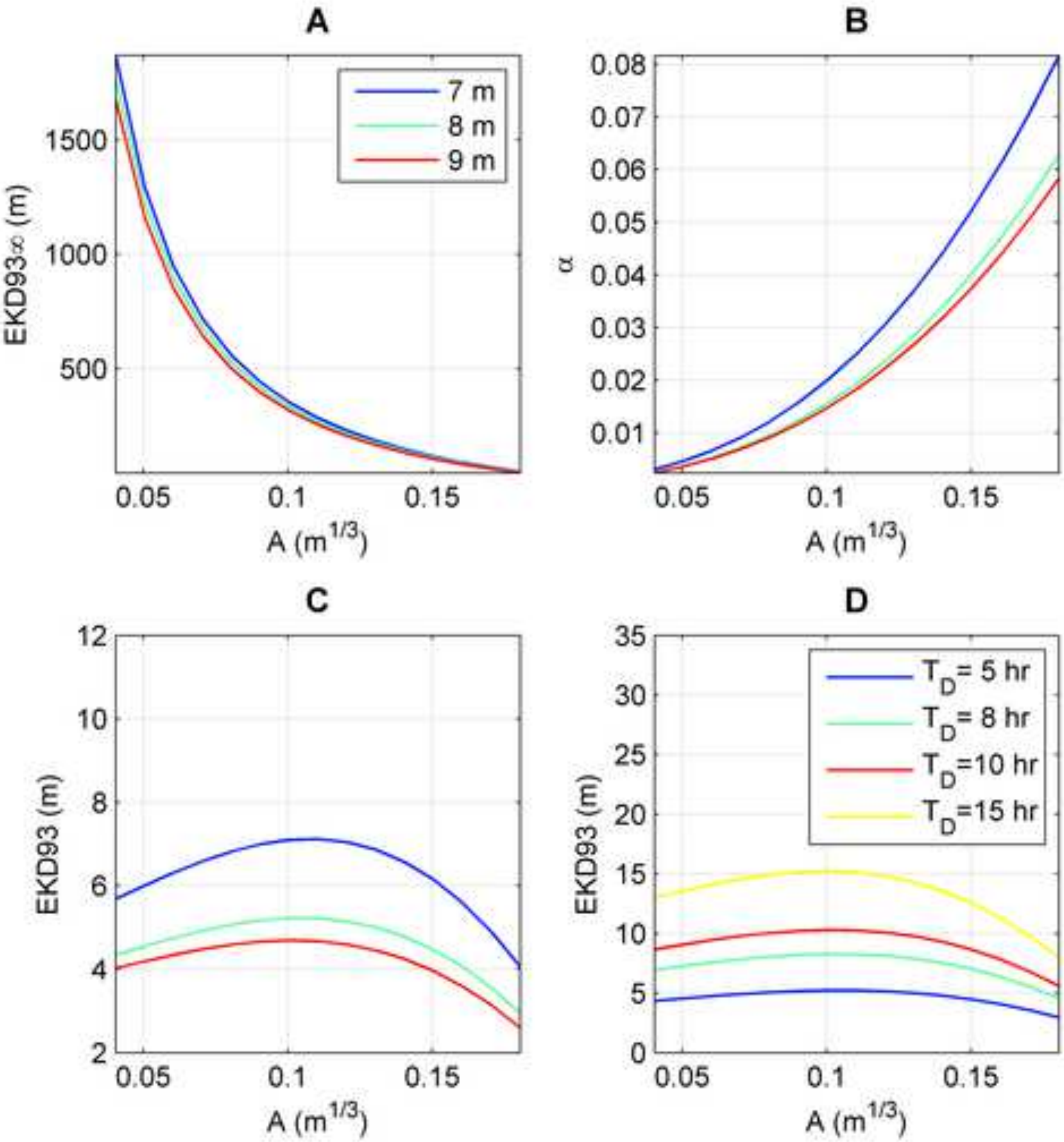
A
7 m
8 m
9 m
EKD93∞ (m)
1500
1000
500
0.05
0.1
0.15
A (m^1/3)
B
α
0.08
0.07
0.06
0.05
0.04
0.03
0.02
0.01
0.05
0.1
0.15
A (m^1/3)
C
EKD93 (m)
12
10
8
6
4
2
0.05
0.1
0.15
A (m^1/3)
D
T_D= 5 hr
T_D= 8 hr
T_D=10 hr
T_D=15 hr
EKD93 (m)
35
30
25
20
15
10
5
0
0.05
0.1
0.15
A (m^1/3)

Figure
Click here to download high resolution image

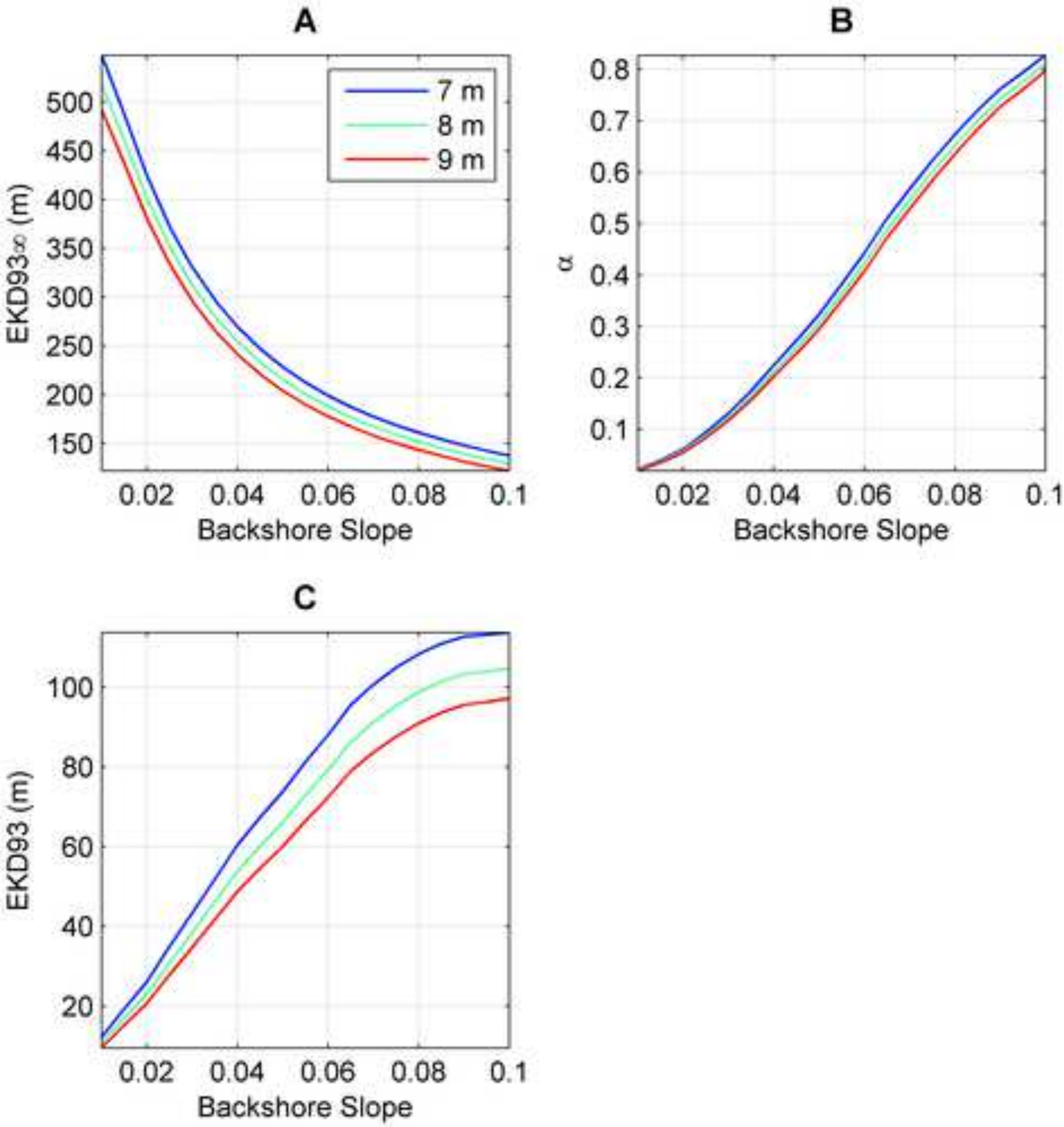

Figure

Click here to download high resolution image

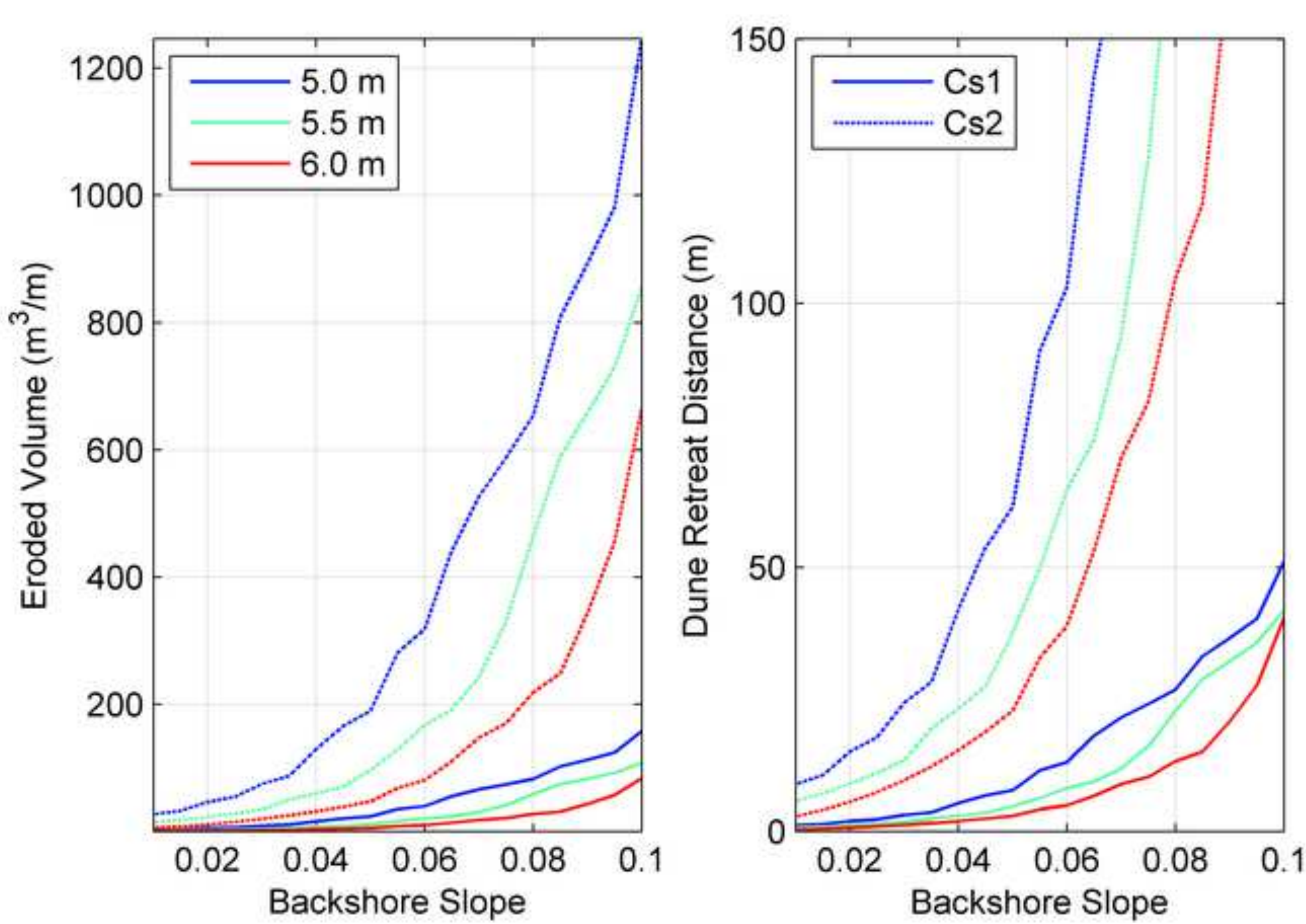

Figure
Click here to download high resolution image

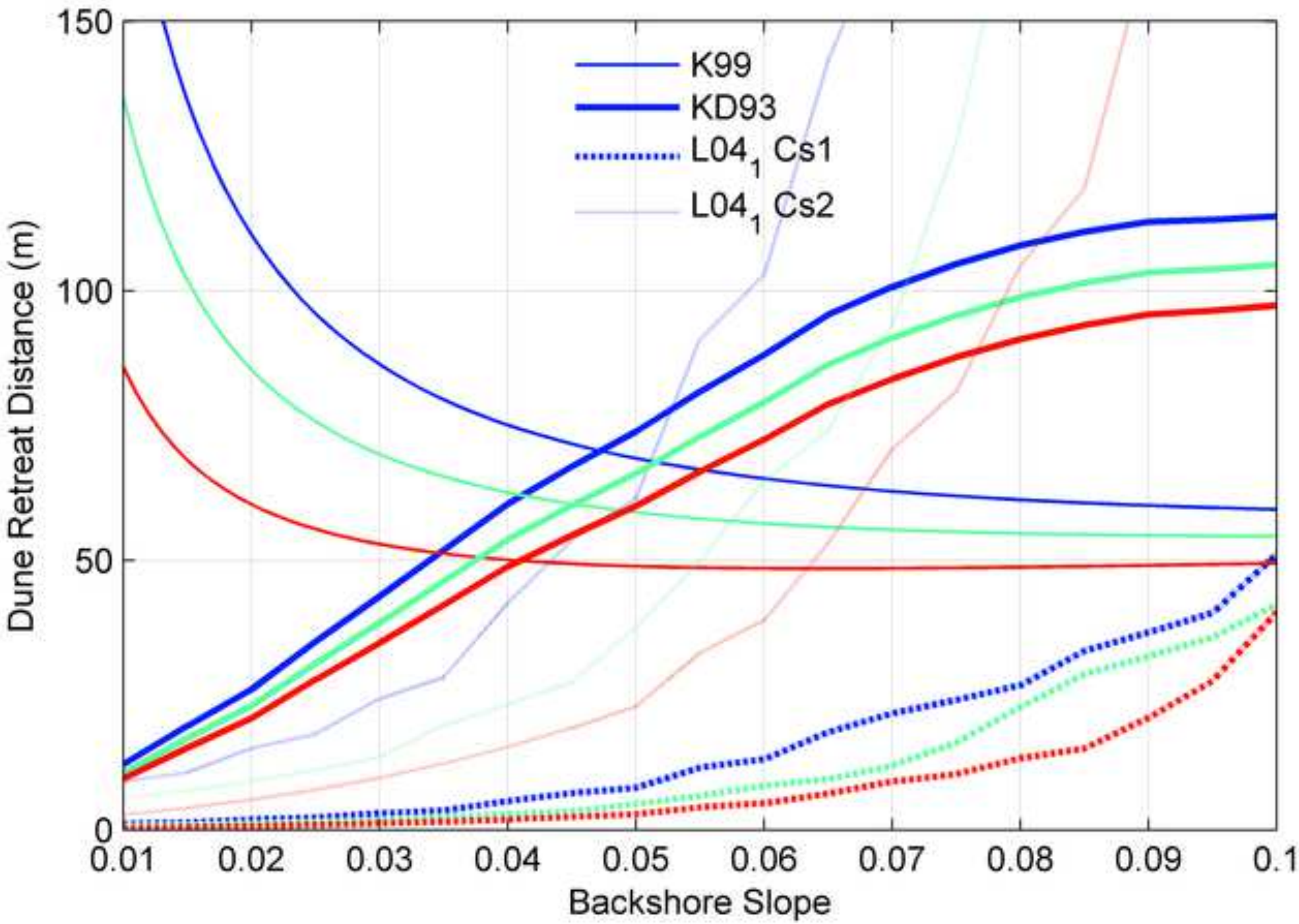

Figure

Click here to download high resolution image

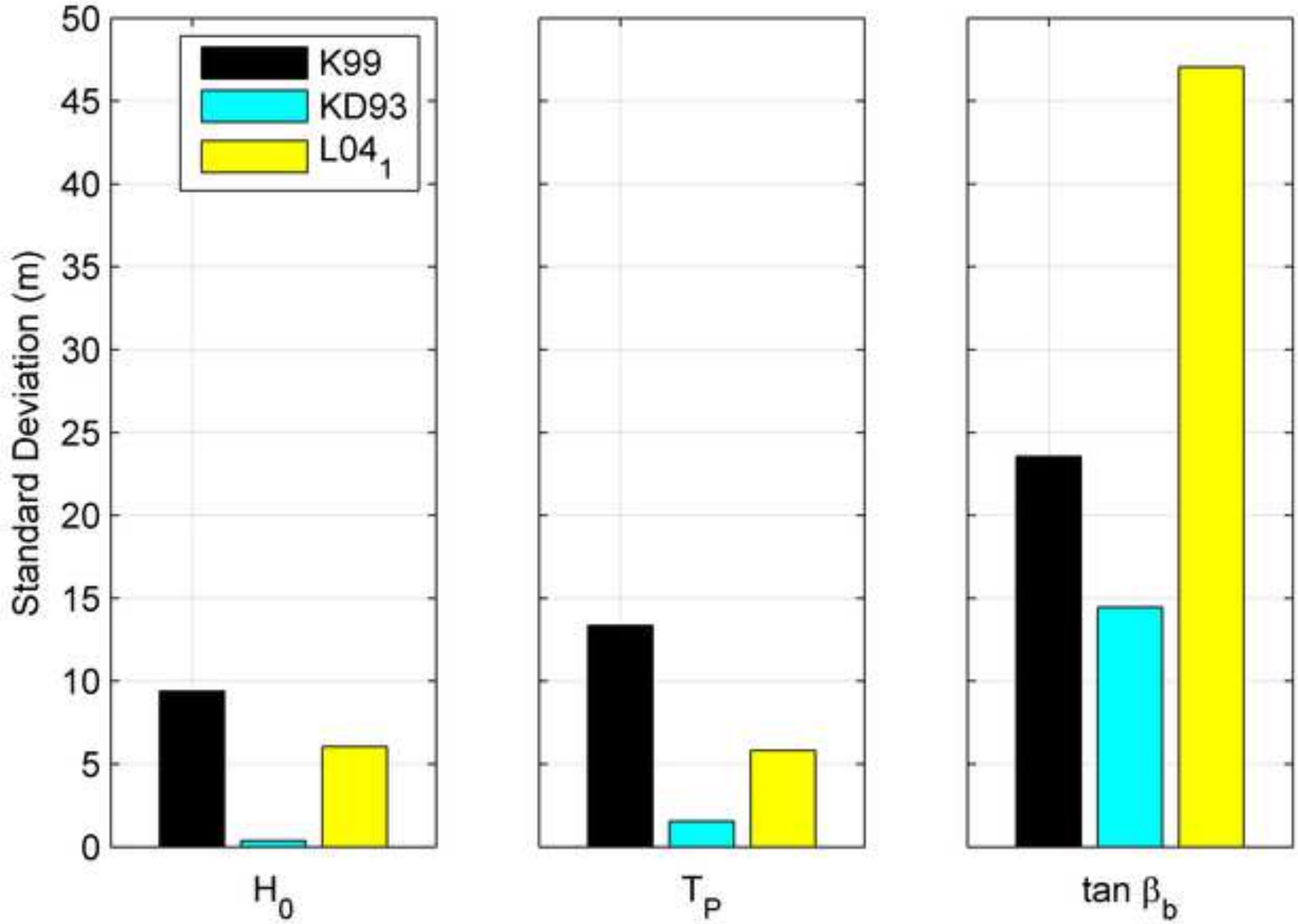

Figure
Click here to download high resolution image

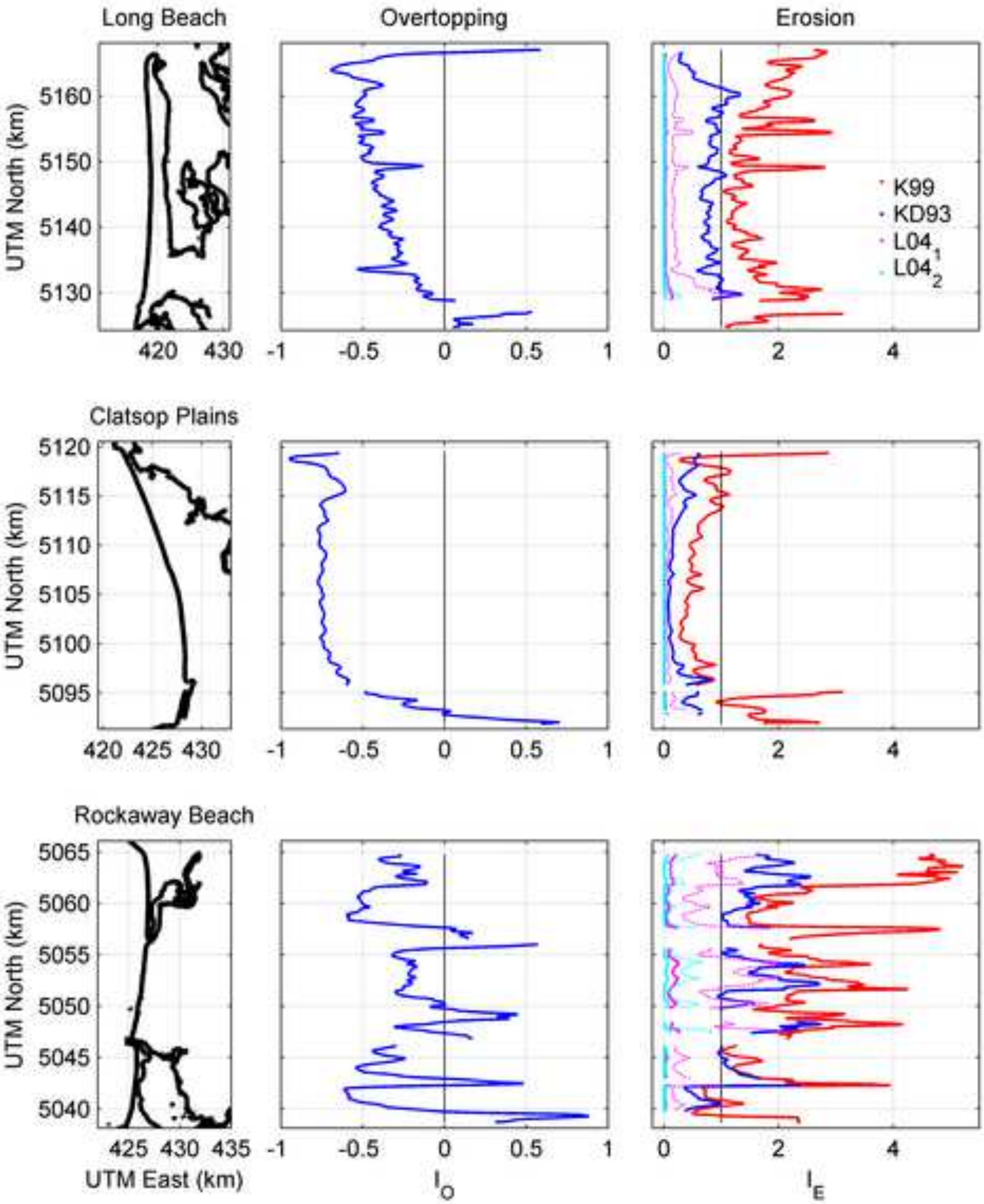

Copyright Form

Click here to download Copyright Form: JCR_Copyright_Release.pdf